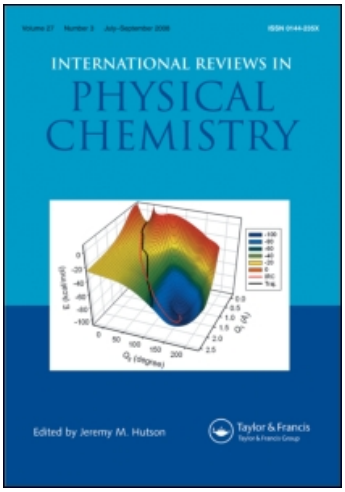

International Reviews in Physical Chemistry
Publication details, including instructions for authors and subscription information:
http://www.informaworld.com/smpp/title~content=t713724383

Transition state in metal atom reactions

J. -M. Mestdagh[a]; B. Soep[a]; M. -A. Gaveau[a]; J. -P. Visticot[a]
[a] Laboratoire Francis Perrin (CNRS-URA-2453), DSM/DRECAM/Service des Photons, Gif-sur-Yvette cedex, France

Online publication date: 26 November 2010

To cite this Article Mestdagh, J. -M. , Soep, B. , Gaveau, M. -A. and Visticot, J. -P.(2003) 'Transition state in metal atom reactions', International Reviews in Physical Chemistry, 22: 2, 285 — 339
To link to this Article: DOI: 10.1080/0144235031000086391
URL: http://dx.doi.org/10.1080/0144235031000086391

INT. REVIEWS IN PHYSICAL CHEMISTRY, 2003
VOL. 22, NO. 2, 285–339

Taylor & Francis
Taylor & Francis Group

Transition state in metal atom reactions

J.-M. MESTDAGH*, B. SOEP, M.-A. GAVEAU and J.-P. VISTICOT
Laboratoire Francis Perrin (CNRS-URA-2453), DSM/DRECAM/Service des Photons, Atomes et Molécules, CEA Saclay, F-91191 Gif-sur-Yvette Cedex, France

The observation of the transition state in metal molecule reactions has been approached by several experimental methods, crossed beams, transition state spectroscopy and more briefly via time-dependent femtosecond localization. The chemistry is far richer than the one-dimensional harpoon model involving an instant single electron jump imagined at the origin.

Contents

*Author to whom correspondence should be addressed. E-mail: jmm@drecam.saclay.cea.fr

International Reviews in Physical Chemistry ISSN 0144–235X print/ISSN 1366–591X online
http://www.tandf.co.uk/journals
DOI: 10.1080/0144235031000086391

1. Introduction

The dynamics of gas phase electron transfer reactions involving neutral metal atoms has been studied for more than 70 years. Since the early work of Polanyi and co-workers, this field has been associated with unravelling the way the transition state (TS) of the reaction is accessed [1, 2]. It is certainly not necessary to recall that the notion of TS is of constant use by chemical physicists, both in gas phase and condensed phase chemistry. The present review is an experimentalist point of view, which aims to show how the continued effort in the study of the dynamics of gas phase metal atom reactions has enlightened the representation of the TS and also vice versa.

Reactions of neutral metal atoms are very attractive in this respect, considering that they often proceed through a fairly localized electron transfer from metal to reactant that defines the TS of the reaction. Hence, only studies concerning neutral systems are reviewed here and no attempt is made to enter the considerable literature on cationic metal reactivity, essentially because the charge on the metal reactant is a complicating factor in the entrance channel of the reaction which leads to the almost ubiquitous formation of strongly bound ion–molecule adducts, before the system accesses the transition state of the reaction. Extensive reviews cover the field of metal cation reactions, when the cation is either naked or ligated [3–7].

Section 2 of the present review is a historical introduction to the TS concept and a presentation of the broader concept that is currently in use, the concept of TS region. As most readers can imagine, this will require the introduction of the notion of movement of the reacting system along the reaction coordinate and as a corollary, movements along coordinates that are perpendicular to the reaction coordinate.

The recent literature concerning reactions of neutral metal atoms has shown that movements along coordinates which, at a first glance, could be considered as perpendicular and uncoupled to the reaction coordinate are often crucial and affect

strongly the dynamics of the reaction. Moreover, this literature shows that the electron transfer cannot be considered as instantaneous. Hence, the remainder of the review is organized about four classes of information that exemplify the evolution toward a more complex representation of the access to the TS region of these reactions.

Section 3 reviews studies documenting the overall movement of the reacting system along the reaction coordinate, from reactants to products over the TS region. This perspective entails the concept of state-to-state experiments with a direct correspondence between the product energy distribution and the reaction path. This section follows also a historical perspective since it starts with the early concept of the harpoon model, a one-dimensional picture which localizes the TS of the reaction where an electron is transferred from the metal atom to the molecular reactant. This section first examines the success of the harpoon model and shows how it must be improved to account for more and more complex situations, in the case where the electron can transfer at different locations or when several electrons are to be transferred. The breakdown of the harpoon model for reactions of ground state transition metals is examined in this section also.

We shall see in section 3 that movements along coordinates that are perpendicular to the reaction coordinate affect the way the TS is crossed, even in situations where the harpoon model was expected to be valid. Section 4 examines this question further. This pertains to the concept of TS spectroscopy (TSS) which directly interrogates movements along perpendicular coordinates and document the coupling between these coordinates and the reaction coordinate. Of course, these movements and couplings are affected by the presence of a reaction medium. This question is examined in section 5 when the reactive medium that supports the reaction is the surface of an unreactive van der Waals cluster. Turning back to reactions in the absence of a reaction medium, real-time experiments offer a unique possibility of documenting wavepacket movements along the reactive coordinate. This pertains to the femto-TSS technique which, so far, has not been used very extensively for metal atom reactions. Corresponding work is reported briefly in section 6. We conclude the review with a series of questions that, in our opinion, are of importance for unravelling the true nature of the TS region in metal atom reactions.

2. The transition state concept: a history

The concept of the TS was formulated as early as 1935 by Eyring [8]. It brings a framework for quantitative predictions of reaction rate constants. The early history of TS theory is provided by Laidler and King [9]. More recently, Polanyi and Zewail discussed the various attempts to observe the TS directly [10]. Recent developments in TS theory have been reviewed very extensively [11]. Finally, the original papers by Eyring [8] and Wigner [12] are put into perspective by Peterson [13] and Garrett [14] respectively, taking the year 2000 as an occasion.

The three major approximations that were at the origin of the TS concept were detailed in a seminal paper by Wigner [12]. The two first can be dropped in the present understanding of TS theory [11, 14], namely the electronic adiabatic character of the reaction and the use of classical mechanics. The third assumption is fundamental and its validation has deserved a considerable literature that is impossible to review here. It concerns the existence of a dividing surface separating the reactant from the products. The key assumption is that a one-dimensional

reaction coordinate can be followed from the reactant valley into the product valley. The potential energy is an extremum somewhere along this coordinate. This defines the TS of the reaction, a saddle point in the potential energy surface (PES) describing the system. Wigner's clarification of TS theory was to define a dividing surface passing through the saddle point, perpendicularly to the steepest descent of the PES, and to assume that all the reactive trajectories must cross this surface, thus defining the crucial deformation of the reacting species which sends them, with no return possibility, into the product valley [14]. Hence the TS appears as the bottleneck between the reactant and the product valleys in the PES. The success of the TS model was to offer the possibility of connecting a bulk quantity, the reaction rate, to the microscopic view of the reacting system provided by quantum mechanics and PES calculations. It may be interesting to note that the same concept of a dividing surface was applied a long time ago to nuclear fission by Bohr and Wheeler [15]

The notion of 'reaction coordinate' that is inherently linked to the TS concept needs a clarification. Consider the simplest situation, that of a reaction involving three atoms:

$$A + B—C \rightarrow A—B + C. \quad (1)$$

The standard concept of reaction coordinate corresponds to a one-dimension movement on the three-dimensional PES describing the (A, B, C) system. It involves the simultaneous deformation of at least two coordinates of the system: the B–C and A–B distances, for example, if it is assumed that the A–C distance and the A–B–C angle remain unchanged during the reaction. This concerted motion of two coordinates breaks the B—C bond, while forming the A–B bond. This corresponds to a curvilinear reaction path on a two-dimensional PES, easy to visualize. In general, because it is hard to believe that the A–C distance and the A–B–C angle play no direct role in the reaction, the reaction coordinate must be imagined as associated with the concerted deformation of the three coordinates characterizing the (A, B, C) system. These two coordinates are regarded as perpendicular coordinates and play an indirect role as defining the breadth of the transition state: the A–C vibration is perpendicular to the reaction path and its stiffness characterizes the width of the transition region. The same is true for the A–B–C angle where a single geometry is rarely preferred; conversely, if the reaction were isotropic on orientation, one could consider the transition region as truly bidimensional. Of course, the reaction coordinate is even more complicated to define when A, B and C are chemical groups rather than atoms. Strictly speaking, if a reactive system with n degrees of freedom is being considered, for the movement along the reaction coordinate to keep its single-dimensional character implies a concerted motion along the remaining n-1 coordinates. This seems hard to achieve when n is quite large, thus suggesting that many degrees of freedom could be weakly coupled, or not coupled at all to the reaction coordinate. In that case, the reaction coordinate could lose, at least partly, its single-dimensional character. This is of course a difficulty and the usual way of bypassing it is to lower the dimensionality of the problem by blocking a geometry (thinking in terms of a collinear reaction in the simplest instance) and to assume that several degrees of freedom do not participate at all to the dynamics of the reaction. The latter just play the role of energy reservoirs and hence act by just changing the level density or the width of the transition region. This route leads to the world of statistical approaches that is the subject of many textbooks, for example that of Baer and Hase [16].

With the time, partly because of the difficulty mentioned just above, the almost mathematical definition of the TS has evolved somehow to become a less stringent concept. Now, the TS appears, especially among the experimentalists, as the more or less extended region, multidimensional by nature, which lies about the reaction coordinate. It corresponds to an ensemble of geometries where the reactive system no longer has the structure of the reactants and not yet that of the products. This new formulation was stated in a very interesting review by Polanyi and Zewail on the quest to visualize the TS region of a reaction [10]. It defines the TS region of the PES as the heart of the chemical reaction, *i.e.* the place where forces enter into play to move atoms and chemical groups within the reactive system. In this picture, the reaction coordinate appears as a minimum energy path which goes from reactants to products, with the reactive system having deformation along coordinates that are perpendicular to the reaction coordinate (in the sense that they do not lead to the reaction directly). In other words, the TS region of the reaction is unbounded along the reaction coordinate, whereas it is bound along the perpendicular coordinates and the reactive system which is transforming from reactants to products undergoes deformations along the perpendicular coordinates.

One point makes metal atom reactions very attractive when exploring the TS region. These reactions usually proceed through an electron transfer, often described by the well-known harpoon mechanism pictured in figure 1. This model, originally proposed by Polanyi [2] to account for exceptionally large cross-sections in alkali atom–halogen molecule reactions, stresses the fact that the electron transfer is possible only for a well-defined geometry of the reactants, simply the Na–Cl_2 distance in figure 1. The very simple harpoon model of the beginning will be examined critically along the review. Anyhow, one point remains. The existence of the electron transfer limits the extension of the TS region. Even if it does not match exactly the picture of a dividing surface as in the early TS concept, the TS region of these reactions is not believed to cover a broad range of geometries, hence opening the possibility of a very extensive study. Furthermore, it provides a simple description of the electron configuration in the TS region, in contrast to purely covalent reactions.

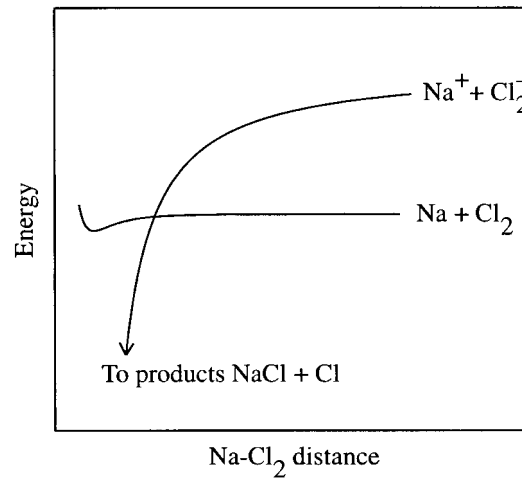

Figure 1. Schematic energy diagram of the harpoon model for describing the $Na + Cl_2 \rightarrow NaCl + Cl$ reaction.

3. Following the path (overall movement) from reactants to products

For simplicity, we first consider a direct reaction, i.e. a reaction that does not involve a long-lived intermediate, and we make the further assumption that a one-dimensional reaction coordinate can be defined. Since the movement of the reacting system in this region implies the simultaneous deformation of several bonds and bond angles, forces and torques appear, which affects the movement of various subunits within the reactive system. The action of these forces will cause a distribution of population over all the degrees of freedom (translational, rotational, vibrational) of the separated products. This involves the transition state seen from the product side: the recoil geometry of the fragments depicts the geometry at the transition state. Also a selective excitation of the reagents will generate a characteristic product energy distribution, thus characterizing a potential energy surface.

This perspective was applied very early to collinear $A + BC \rightarrow AB + C$ reactions when the so-called Polanyi's rules were developed [17–20]. These rules connect the location and height of the energy barrier controlling the reaction to the dynamics of the reaction and ultimately to the energy distribution of both the reactant and the reaction products. The dynamical approach of Polanyi and co-workers was constructed on very general PESs, with no reference to a particular process. The same methodology is currently being revisited in order to help in understanding the global shape of the product energy distribution in indirect three-atom reactions going through the temporary formation of a collision complex [21–24]. Of course, these very general approaches apply to any class of gas phase reaction, including the present metal atom reactions.

3.1. *The 'Harpoon model', a one-dimensional picture of reactions with a single active electron*

The study of numerous oxidation reactions of alkali atoms [20, 25–36] has been conducted in the light of the passage via a single-dimensional trajectory involving an electron transfer step (harpoon) that represents the transition state of the reactions. The early literature leads to the concept of this 'harpoon mechanism' that is illustrated by figure 1 for the reaction

$$Na + Cl_2 \rightarrow NaCl + Cl. \tag{2}$$

It applies to any reaction of the type

$$M + AB \rightarrow M^+ \cdots AB^- \rightarrow M^+A^- + B, \tag{3}$$

where M acts as an electron donor and the moiety A of the molecular reactant AB as an acceptor. The 'harpoon model' was first proposed by Polanyi [2] and put in a semiquantitative form by Magee [37]. Gislason has reviewed the early efforts to make it quantitative [38]. According to this model, the reaction of ground state Na with Cl_2 proceeds through a long-range electron transfer from the highest occupied molecular orbital (HOMO) of Na (or more generally metal M) into the lowest unoccupied molecular orbital (LUMO) of Cl_2 (or more generally AB in reaction (3)), forming the $Na^+Cl_2^-$ (or M^+AB^- in reaction (3)) complex, the TS of the reaction, which falls apart as $Na^+Cl^- + Cl$ ($M^+A^- + B$ in reaction (3)).

At this point, when following the terminology of Truhlar, the harpoon mechanism appears as an entrance-channel model in a single-surface reaction [39]. It defines the TS region of the reaction as the electron transfer region with the further assumption that neither the geometry nor the electronic properties of the molecular

reactant are changed when the metal atom is approaching. Hence, the reaction dynamics is determined by the switch at the electron transfer distance between the entrance coordinate where no deformation of the molecular reactant occurs and the exit coordinate where the negatively charged molecular ion falls apart to form the reaction products. From this, three parameters control the dynamics of the full reaction.

(1) *Electron transfer distance*. The electron transfer occurs at the $M \cdots AB$ distance R_c where the ion-pair potential $M^+ \cdots AB^-$ (assumed to *depend only on* the $M^+ \cdots AB^-$ distance) crosses the covalent curve $M \cdots AB$. Assuming a flat covalent curve and R_c to be large enough for the Coulomb interaction to be dominant in the ion pair, the crossing distance is given by the Magee formula [37]:

$$R_c = \frac{14.4}{IE - EA} \tag{4}$$

where R_c is expressed in Å and the energies IE and EA in eV, IE being the ionization energy of the electron donor M and EA the electron affinity of the acceptor AB. This expression could be refined [38], but it is often enough to predict the important aspects of the reaction. It is historically very important since it gives an upper limit of the total cross-section of a pure harpoon reaction and was able to account for the very large cross-sections measured in the oxidation reaction of alkali atoms by halogen molecules [2].

(2) *Stability of the molecular anion in the exit valley*. The dynamics that follows the formation of the electron transfer complex M^+AB^- is markedly dependent on the stability of the AB^- anion. When stable as in the case of NO_2^- in the $Cs + NO_2$ reaction, the $Cs^+NO_2^-$ charge transfer complex survives for many rotations and the reaction product CsO presents a characteristic forward–backward symmetry in the angular distribution [26, 40]. Grice has derived a microcanonical theory of reactions decaying from a such persistent complex [41]. When the AB^- anion is not stable with respect to the dissociation as $A^- + B$, the charge transfer complex dissociates before it has had time to rotate. The reaction is called direct. The reaction product is forward scattered when the AB^- molecular anion is formed close to its dissociation limit and requires the Coulomb field of the positive ion M^+ to be dissociated. The reaction is then described by the spectator striping model. In contrast, when AB^- evolves along a very steep repulsive potential, the reaction product is backward (rebound reaction) or sideways scattered [31, 42].

(3) *Polarization effects in the electron transfer step*. The HOMO and the LUMO involved in the electron transfer step are non-spherical orbitals in general. Hence, their relative orientation should play a role in the access to the TS region of the reaction. An important branch in reaction dynamics is therefore dynamical stereochemistry (also called stereodynamics) [43] which interrogates the effect of orienting or aligning the reactant in space, in order to guess which relative orientation of the HOMO and the LUMO is best to access the TS region of the reaction.

Among these characteristics, the last two go beyond the pure one-dimensional picture of the early harpoon model.

3.2. *A simple multidimensional model of the TS region of reactions with a single active electron*

Several simple classical models have been proposed to account of metal atom reaction, beyond the simple harpoon picture [39, 44]. One is particularly attractive because it includes very simply the three characteristics of the TS region listed in the previous section, namely the direct interaction with product repulsion (DIPR)–distributed as in photodissociation (DIP) model, which predicts an entire range of dynamical observables: angular and recoil velocity distributions, rotational and vibrational energy of the reaction products.

The model, under the simple form DIPR, was originally proposed by Kuntz and co-workers [45–48]. It is pictured in figure 2 and is founded on the following assumptions:

- AB is initially in the ground rotational and vibrational level and the M + AB system evolves on an essentially flat potential surface. This initial movement is assumed to have a negligible effect on the subsequent reaction dynamics, an assumption which fits with complete decoupling between the approach coordinate and the other coordinates of the system. This is probably a valid first approximation when the electron jump distance is large, but might become questionable in other circumstances, for instance for rebound reactions when the electron jumps at closer approach distances. We shall see an effect of this when discussing below the $K + CH_3I \rightarrow KI + CH_3$ reaction in the light of [49]. In fact, a leitmotiv in this review is to show that the separability between the approach coordinate and the other coordinates is definitely too crude an approximation when reaction dynamics is considered in some detail. In the present step, since separability is still assumed, energy levels of M and M^+ are those of the unperturbed atom and ion. Similarly, potential curves of AB and AB^- are those of the free molecule and of the free molecular anion.

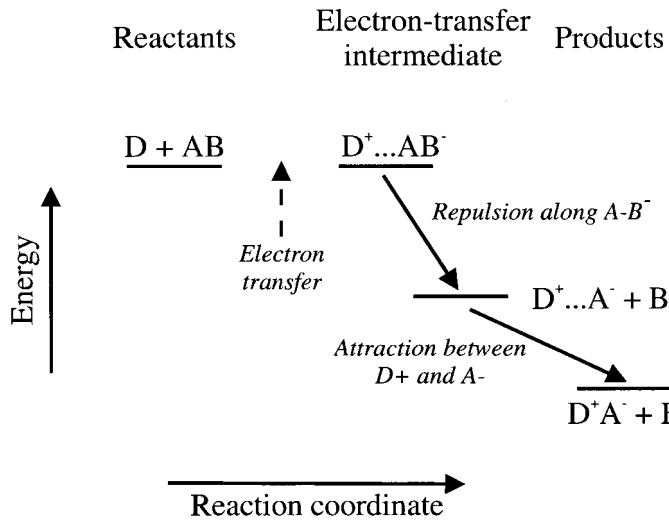

Figure 2. Schematic description of the energy release according to the DIPR-DIP reaction mechanism.

- The electron jump forming the complex $M^+ \cdots AB^-$ takes place at the distance R_c given by the Magee formula. A probability parameter depending on the M–A–B angle can easily be introduced at this point to account for stereodynamical effects.
- As said above for the early harpoon model, the reaction is initiated by the sudden change of coordinate that follows the electron jump and turns on the repulsion between A^- and B.
- If it is considered that the R_c distance is large (see the first item above), no interaction is assumed between M^+ and the departing B moiety, but, owing to its long-range character, the attractive interaction between D^+ and A^- is considered. The subsequent angular and energy distributions of the product MA are assumed to be determined by the monotonic energy release along the $A^- - B$ coordinate and the attraction between M^+ and A^-. The attractive and repulsive energy releases are assumed to be separable, and the attraction is assumed to be slower than the repulsion.

The DIP extension to the model was proposed by Herschbach to provide the necessary empirical basis for estimating the repulsive interaction between A^- and B [50]. It considers that the electron attachment to the AB molecule is mostly a vertical process and that the subsequent dissociation into A^- and B mimics photodissociation. The mathematical expressions relevant to the model are given by Truhlar and Dixon [39]. Zare and co-workers have extended the model to chemiluminescent reactions and a full account of the new model is given in [51]. It was used to predict successfully the product state distribution in the reaction $Ca(^1S_0) + F_2 \rightarrow CaF(B\,^2\Sigma^+) + F$.

The DIPR model is often used to help in understanding the stereodynamics of direct reactions [52–55]. The important parameter of the model is thus the electron transfer probability as a function of the molecular orientation. The same parameter, which actually defines the best geometry of the system at the electron transfer step, also plays a role in determining the product alignment in chemiluminescent reactions [56, 57]. A new model has been introduced recently, the anisotropic impulsive model [58]. It is conceptually close to the DIPR model and also helps to determine the preferred angle of approach between the reactants.

3.3. *Dynamical effects associated with changing the electron transfer distance*

The electron jump distance R_c depends on the ionization energy IE of the metal atom (see equation (4)). A way of increasing R_c is therefore to lower IE by exciting the metal atom electronically. This has been achieved in the group of Lee when investigating reactions of excited of sodium with halogen-containing molecules. These studies can be summarized under three items, whether the reaction proceeds from a rebound, a spectator stripping or an intermediate mechanism.

- *Rebound reaction.* The reaction of ground state sodium,

$$Na + CH_3Br \rightarrow NaBr + CH_3, \tag{5}$$

is a classic example of rebound reaction, with 84% of the product NaBr scattered in the backward hemisphere. This arises from two factors: a close approach between Na and CH_3Br for the electron transfer to proceed and a steric effect, where sodium must approach the Br end of CH_3Br to bounce back

as NaBr. The latter point corresponds to the well-known concept of acceptance angle for a reaction [59].

When exciting sodium electronically to the $3p\,^2P$ level and higher to $4d\,^2D$, the reactive cross-section increases and the centre-of-mass angular distribution widens. It still corresponds to the rebound mechanism with 79% of the reaction product in the backward hemisphere for reaction of $Na(4d\,^2D)$. This suggests that the acceptance angle of the reaction widens [60], a result that is interpreted below in the light of a recent re-interpretation of the mechanism of the reaction $K + CH_3I \rightarrow KI + CH_3$, another rebound reaction [49].

The origin of the acceptance angle in the $K + CH_3I \rightarrow KI + CH_3$ reaction has been re-examined in [49]. The starting point of the new interpretation is that localization of the electron transfer at a well-defined distance R_c between the reactants is too crude an approximation when the molecular reactant does not have a large positive electron affinity. The more correct picture would go along the bond-stretch model, a model originally introduced to account for the quenching of $Na(3p\,^2P)$ by molecules of negative electron affinity (N_2 and H_2) [61]. In that case, the approach between K and CH_3I would result in a partial and progressive electron transfer from K to CH_3I, hence inducing the progressive elongation of the CH_3—I bond.[1] The two important inputs of the interpretation are first that the time needed for the elongation is comparable with the collision time and second that the stereodynamics of the reaction stems from the ease of the final, full electron transfer. The more the CH_3—I bond has had time to elongate, the easier the final electron transfer which promotes the reaction. Hence, the longer is the distance at which the electron jump occurs and the less restrictive are the geometry requirements which favour the final, full electron transfer. In other words, the acceptance angle of the reaction is wider when the C—I bond has time to stretch. It is important to notice that, with this interpretation, the reaction does not follow the approach of the reactants along a single coordinate, the distance between the metal atom and the molecular reactant. Instead, it implies the coupling between an internal coordinate of the molecular reactant (the C—I bond) with the approach coordinate of the metal atom. This is the first appearance of the leitmotiv mentioned above, that separability between the entrance coordinate and other coordinates is too crude an approximation.

With this interpretation, the observations recalled above on the effect of increasing the electronic energy of sodium in the $Na + CH_3Br \rightarrow NaBr + CH_3$ reaction become clear. The excited orbitals of sodium become more and more diffuse when switching from $3s\,^2S$ to $3p\,^2P$ and $4d\,^2D$. Hence the initial partial electron transfer occurs at larger and larger distances and this allows more and more time for the CH_3Br molecule to stretch. From above, this is likely to relax the steric requirements for the final full electron transfer which promotes the reaction, in agreement with the experimental observations. It appears here that the saddle point is becoming a large ridge alongside the angular coordinate. Nevertheless, this breadth does not cause the movement across the transition state to be multidimensional since the

[1] Notice that electron transfer, when partial, cannot be distinguished clearly from orbital polarization.

orientation is not the driving force to pass the saddle point. On the other hand, the bond stretch needed for the electron transfer can make the passage of the transition region multidimensional if the potential gradient induced by the bond stretch on the electron accepting group is significant. It is clear that the transition region has to be defined as a broad region different from the reagents or products.

- *Spectator stripping reaction.* The reaction $Na + Cl_2 \rightarrow NaCl + Cl$ proceeds from the spectator stripping mechanism. Experimentally, the electronic excitation of sodium has little effect on both the reaction cross-section and the angular distribution of the product NaCl. This is understandable considering that the electron jump distance R_c predicted by the Magee formula is very large, 5.22 Å, for ground state Na and 22.3 Å when sodium is excited to the $3p\,^2P$ level. In fact, the electron jump that promotes the reaction does not proceed at such large distances because of a poor overlap between the sodium HOMO and the Cl_2 LUMO. Presumably, the actual electron jump distance (TS) does not change significantly when exciting sodium to the $3p\,^2P$ level [60, 62].
- *Intermediate case.* The reaction

$$Na + HCl \rightarrow NaCl + H, \qquad \Delta H = +0.2\,eV, \tag{6}$$

is endoergic with ground state sodium and still has a small cross-section at collision energies above threshold. It is turned on when sodium is excited electronically. Its mechanism has been documented for excitation to $3p\,^2P$, $4d\,^2D$ or $5s\,^2S$ [62–64].

The NaCl product is backward scattered and has a broad velocity distribution in the reaction of $Na(3p\,^2P)$. The observed velocity and angular distributions of NaCl can be fitted by adjusting the empirical stereodynamics parameter of the DIPR-DIP model (see section 2), allowing one to draw two conclusions: (i) almost no preference on the HCl orientation at the moment of the electron jump, with only a slight preference for the Na $\cdots$ Cl approach; (ii) a partial breakdown of the basic DIPR–DIP assumption, which separates the breakage of the H—Cl bond from the formation of the Na—Cl bond. This suggests a certain degree of concertedness to the reaction (as above in the $Na + CH_3Br$ reaction), essentially because the electron jump distance is not very large (3.7 Å). In addition, the fact that the NaHCl system is packed closely in the TS region, a bit like a compressed spring, explains also the large energy release into translation after the reaction [63].

Excitation of sodium to the $4d\,^2D$ and $5s\,^2S$ levels, puts *c.* 4 eV electronic excitation in the system, versus *c.* 2 eV with the $3p\,^2P$ excitation. Although the system contains more energy, the experiment reveals that the translational energy release between the products is smaller in the $Na(4d\,^2D)$ and $Na(5s\,^2S)$ reactions than in the $Na(3p\,^2P)$ reaction, indicating that most of the available reaction goes as vibrational excitation of the product NaCl. This can be rationalized by considering that the additional 2 eV of electronic excitation has moved the electron jump distance to 8 Å and the Na–H–Cl system is no longer packed at the TS. Nevertheless, the reaction mechanism has not reached the spectator stripping limit, since the product NaCl is mostly backward scattered [62, 64].

3.4. *Dynamical stereochemistry*

Non-spherical molecular reactants or metal atom reactants, when excited to a P (or D) level, can be polarized, either oriented or aligned, with respect to the relative velocity vector of the collision. Studies documenting the effect of varying this polarization with regard to the reaction pertain to vector correlation in reaction dynamics [65–69].

The previous section gave an example of such a correlation, that between the alignment of the molecular reactant CH_3Br and the angular distribution of the product NaBr in a situation where the molecular alignment is selected by the electron transfer step, in the $Na^* + CH_3Br$ reaction. The present section discusses situations where either the molecular reactant or the atomic reactant when electronically excited becomes polarized in the laboratory reference frame, prior to collision with the other reactant.

- *Charge separation processes*. Before discussing studies on reactive collisions *stricto sensu*, we examine a situation where the electron transfer step can almost be isolated, namely the formation of an ion pair in hyperthermal collisions. Such experiments were conducted by the group of Brooks, where ground state potassium atoms are collided in a crossed-beam apparatus with spatially oriented CH_3CN molecules at energies ranging between 5 and 30 eV, i.e. large enough for the charged species to separate after the collision when the K atom has transferred its valence electron to the acetonitrile molecule [70–72]. It was observed that the most abundant negative ion, CN^-, is preferentially formed on attack at the CN end of the molecule, whereas the CH_2CN^- ion is observed at large collision energies with attack at the CH_3 end. These authors tentatively rationalized the observation by assuming that the CN^- production results from an initial electron transfer into the LUMO with antibonding π^*_{CN} character, presumably followed by the bend of the CCN angle and population of the σ^*_{CC} antibonding orbital which stimulates dissociation as CN^- [72].
- *Reactions of oriented molecules*. Such preference in molecular orientation for the electron transfer has its counterpart in reaction dynamics and has been extensively documented for reactions of alkali atoms with symmetric top molecules oriented by hexapole electric fields in the groups of Brooks [73–76], Bernstein [49, 59, 77–82], and Stolte [83–92] and for reactions of alkali atoms with oriented dipolar molecules (in high constant electric fields) in the group of Loesch [52–54, 93–95]. A case study is the $K + CH_3I \rightarrow KI + CH_3$ reaction, which has been revisited very recently [49]. These experiments have led to the notion that in rebound reactions, when an activation barrier has to be overcome for the reaction to proceed, the height and location of the barrier depend on the angle of attack of the metal atom on the molecular reactant [59, 74, 80, 84, 88]. The connection of this with the TS theory of thermal reactions has been examined carefully [96–98]. The recent re-interpretation of this reaction has shown that the effect of orienting the CH_3I molecule cannot be understood without coupling the motion along the K–CH_3I approach coordinate with progressive stretching of the C—I bond in CH_3I [49].
- *Reactions of polarized atoms*. An important development in stereodynamics concerns reactions of electronically excited metal atoms that are not in an S state. In that case, the electron transfer step may depend on the polarization of

the excited orbital. Achievements in this field mostly concern reactions of alkali [99–101] and alkaline earth [56, 102–106] atoms.

One of the first observations concerns the chemiluminescent reaction of electronically excited $Ca(4s4p\ ^1P_1)$ with chlorine-containing molecules. The branching ratio between the $CaCl(A\ ^2\Pi)$ and $CaCl(B\ ^2\Sigma^+)$ chemiluminescence signals was found to be reminiscent of the initial alignment of the 4p orbital, a result that was interpreted by assuming that the chemiluminescent reaction is induced by the transfer of the inner electron, 4s, thus allowing the outer electron, 4p, to transport the electronic excitation and the alignment into the product CaCl [102, 103]. The question of outer and inner electron transfer is examined further in section 3.5 within the framework of the 'multilocation harpoon' mechanism.

Another example is the crossed beam study of the reaction [99]

$$Na(4d\ ^2D) + HCl \rightarrow NaCl + H. \quad (7)$$

It was found that the reaction is favoured when the d_{z^2} orbital of sodium is aligned along the relative velocity vector of the collision and that the optimum alignment varies only slightly with the scattering angle of the product NaCl.

Before the interpretation of these experiments is given, attention must be drawn to the following difficulty. The orbital preparation is performed in the laboratory reference frame at infinite separation between the reactants. At finite distances, a transition is made to the molecular frame alignment and several possible electronic configurations can be then reached when the system is close to the TS region. This difficulty refers to the concept of locking radius, which deals with the locking of orbitals to the rotating molecular frame in the course of a collision [107, 108]. With this in mind, it has been concluded from the experimental observation that the reaction $Na(4d\ ^2D) + HCl \rightarrow NaCl + H$ goes through a long-range electron transfer (see section 3.3) and that the Na–HCl axis dominates over the Cl–H axis in determining the most favourable alignment angle. In other words, the d_{z^2} orbital of sodium just needs to be pointing towards the HCl molecule for the reaction to proceed, but the Na, Cl and H atoms do not need to be collinear at the transition state [99]. Of course this picture complements that drawn in section 3.3 when discussing reactions of electronically excited sodium.

Measuring the polarization of the reaction products is also an important issue in stereodynamics. Much of the activity in this field concerns the reactivity of alkaline earth atoms since the corresponding reaction products are easy to probe by optical techniques. A full account of the way to measure product alignment and orientation in bimolecular collisions has been given by Orr-Ewing and Zare [109]. Such measurements, with the help of simple models such as the DIPR–DIP model seen in section 3.2, give insight into the shape of the reactive system at the moment where forces are released [56, 57, 110–113].

3.5. *'Multilocation harpoon' and 'Double-harpoon' mechanisms*

Alkaline earth atoms have fairly low ionization potentials, as alkali atoms (for example, 5.21 eV for barium versus 5.14 eV in sodium [114]). Hence the reactions of alkaline earth atoms with oxidizing molecules are also initiated by an electron transfer and should follow the harpoon mechanism. However, alkali atoms are monovalent species, whereas alkaline earth atoms have two valence electrons.

Because of this, two effects are expected, which depend on whether the reaction product is monovalent or divalent. In the latter case, a doubly charged product, BaO ($Ba^{2+}O^{2-}$) for example, has to wait for the transfer of the two valence electrons of barium to be formed in a $Ba + O_2$ reaction [115]. The corresponding mechanism is called a 'double harpoon' in the following. In the case discussed in the preceding sections, the formation of the reaction product involves the transfer of a single electron, but the presence of the second valence electron opens up the possibility of chemiluminescent reactions, especially in the case where the product is ionic, BaCl (Ba^+Cl^-) in the $Ba + Cl_2$ reaction for example. In that case, the electronic excitation of the product corresponds to electronic excitation of the remaining valence electron in the metal ion Ba^+ moiety of the product. Branching to this situation has been interpreted as due to a harpoon mechanism with electron transfer, not at the outer crossing between the $Ba + Cl_2$ covalent and ground state $Ba(6s)^+ + Cl_2^-$ curves but at an inner crossing between the covalent curve and a $Ba^{+*} + Cl_2^-$ excited ion-pair curve [102, 103, 116, 117]. The fact that the electron transfer may arise at various places along the covalent curve, to form either ground state or excited state ion pairs, is referred to as a 'multilocation harpoon' hereafter.

Reactions of ground state alkaline earth atoms have been the subject of too many studies to be reviewed extensively. A comprehensive compilation of studies prior to 1988 has been provided by Menzinger [117]. This review mostly concerns chemiluminescent and chemi-ionizing metal–halogen reactions. Many other references can be found in earlier review papers and book chapters [27, 116,118]. The present review focuses on a few studies that clarify the 'double-harpoon' and 'multilocation harpoon' mechanisms and examines the competition between them both.

3.5.1. *The 'multilocation harpoon' model*

Most reactions of alkaline earth atoms with halogen-containing molecules forming a metal halide product have been studied [104, 116, 117, 119–126]. Consider the particular reaction

$$Ba + Cl_2 \rightarrow BaCl + Cl, \qquad \Delta H = -2\,eV. \tag{8}$$

The ground state product BaCl has the structure Ba^+Cl^-. A single electron is transferred from barium to chlorine and correlates adiabatically with the single-electron transfer intermediate $Ba^+Cl_2^-$. Experimentally, the reaction mechanism appears as close to the spectator stripping limit, with the product BaCl scattered in the forward hemisphere, as in the corresponding alkali + Cl_2 reaction [120]. At this step, reaction (8) appears as typical example of a harpoon reaction in its simplest form.

The reactions of alkaline earth atoms with halogenated molecules, of which reaction (8) is an example, are exoergic enough to give access to chemiluminescence channels, especially when the metal atom is excited electronically. Continuing with the example of reaction (8), the chemiluminescent product BaCl has also the structure Ba^+Cl^- and its electronic excitation is localized on the metal ion. Hence, the perturbation of the electronic states (ground and electronic states) of the newly formed BaCl molecule by the departing Cl moiety is expected to be similar and not much coupling between them that could account for the branching to the chemiluminescence is to be expected in the exit valley of the reaction. Hence, Zare and co-workers for the Ca + HCl, Cl_2 systems [102, 103] and later Menzinger for the $M + X_2$ systems (M = alkaline earth atom, X_2 = halogen molecule) [116, 117] have

looked at an entrance channel effect for the interpretation of the branching to chemiluminescence. They suggested the picture that branching to chemiluminescence is due to a 'multilocation harpoon' where the electron transfer occurs at an inner crossing between the flat covalent curve and an ion pair curve correlating with the electronically excited alkaline earth ion M^{+*}. Menzinger has examined carefully the crossing and anticrossing question between the covalent $M + X_2$ curve and the various $M^{+*} + X_2^-$ curves in terms of molecular state symmetry [117]. This has defined a network of conical intersections in the perpendicular and the collinear approaches between the reactants and a model has been built from this network, which allows for electron transfer at various approach distances, and for various relative orientations of the reactants. A further empirical rule has been introduced by Menzinger to predict the efficiency of the couplings: the projection M_L of the M^{+*} electronic angular momentum onto the $Ca \cdots X_2$ axis is transferred in the molecular product M^+X^- as the Ω projection of the electronic angular momentum which defines molecular states. In this form, the model has allowed a variety of observations concerning the branching ratio into the molecular states of the product MX [117], their dependence on the collision energy and polarization effects in the $Ca^* + HCl,\ Cl_2$ reactions [102, 103] to be accounted for.

The above success of the 'multilocation harpoon' model suggests that the electronic structure of M and M^+ in the electron transfer region, representing the TS region also, is far from that of the free atom or free ion. Consider for instance the chemiluminescent reaction $Ca + F_2 \rightarrow CaF^* + F$. The state correlation diagram drawn by Menzinger implies the transformation of $Ca(4s^2\ ^1S).F_2(^1\Sigma_g^+)[^1A']$ into $Ca^+(4p\ ^2P).F_2^-(^2\Sigma_u^+)[^1A']$. When considering these molecular states in terms of localized atomic orbitals with a single configuration, the transformation indicates that, when the 4s electron of calcium is transferred to the fluorine molecule, the other 4s electron of calcium is transformed as the 4p electron of Ca^+. Clearly, for such a transformation to be efficient, s and p atomic orbitals of calcium, or those of the calcium ion, or both, must be strongly hybridized in the electron transfer region as suggested by Field and co-workers in their ligand field description of the calcium monohalide molecules [127].

Hence we are quite far from a picture where the metal atom approaches from the molecular reactant, fairly unperturbed, until a sudden electron transfer occurs.

We are again in a situation where the picture of a sudden and localized electron transfer must be replaced by that of a more extended TS region where atomic orbitals are perturbed, prior to the electron transfer, thus accompanying changes in the bonding of the molecular partner. We already saw such a situation in section 3.4 for the rebound reaction $K + CH_3I \rightarrow KI + CH_3$, the dynamics of which was revisited in [49]. Importantly, the new interpretation of the dynamics of this reaction introduces a time-scale consideration: the electron transfer (and consequently the reaction) has a larger probability when the molecular reactant has had time to stretch during the collision.

A related time-scale limitation has been considered within the 'multilocation harpoon' model by De Castro *et al* [128, 129] to account for translational energy effects in crossed-beam studies of chemiluminescent reactions [128, 130, 131]:

$$\begin{aligned} Ca(4s3d\ ^1D_2) + HCl &\rightarrow CaCl(A\ ^1\Pi) + H, \\ Ca(4s3d\ ^1D_2) + HBr &\rightarrow CaBr(A\ ^1\Pi,\ B^1\Sigma^+) + H. \end{aligned} \tag{9}$$

These authors estimate that the reaction occurs only if the ion pair complex has had enough time to rearrange during the time τ associated with the non-adiabatic transition from the covalent curve to the ion pair curve [128, 129]. In quantifying the coupling matrix element between these two curves and the rearrangement time of the charge transfer complex necessary to promote the reaction, they were able to reproduce quantitatively the dependence of the chemiluminescence signals on the collision energy.

At first glance, τ as the limiting time-scale is not very satisfactory and a better choice could be the time τ_{ionic} that the system is allowed to spend on the ion-pair curve to promote the reaction before back-donation of the electron to the metal can occur in the exit valley of the collision. In fact τ and τ_{ionic} are two valid limiting time-scales. They simply refer to two different limiting cases. τ_{ionic} is the limiting factor when the electron attachment to the molecule does not necessitate a deformation of the neutral molecule. In that case, the dynamical limitation comes from the molecular anion when it is slow to dissociate. In contrast, when the neutral molecule cannot attach an electron, without a prior deformation, then the time τ is the dynamical parameter to consider.

The relevance of a time-scale based on τ_{ionic} is illustrated by the following spectacular observation in non-reactive collisions between caesium and O_2 at hyperthermal collision energies (25–100 eV) [132–135]:

$$Cs + O_2 \rightarrow Cs^+O_2^- \rightarrow Cs + O_2. \tag{10}$$

The initial electron transfer forms the anion O_2^- with the bond length of the neutral molecule, shorter than that of the anion. Hence the newly formed O_2^- is compressed and starts to oscillate with a period of 3×10^{-14} s. At the chosen collision energy, depending on the impact parameter, the collision time varies between 0.5 and 3 times the vibration period. As a result, there is a family of impact parameters where O_2^- is back in position to return the captured electron on the exit channel of the collision, for the formation of $Cs + O_2$ to be observed. There is another family also, for which the electron return is impossible. In that case the collision leads to chemi-ionization and to the formation of $Cs^+ + O_2^-$ instead of $Cs + O_2$. Because of the missing impact parameter, oscillations are observed in the angular distribution of the Cs atoms, the oscillation period being related to the vibrational period of O_2^-.

The time limitation used by De Castro *et al.* [128, 129] to account quantitatively for reactions (9) is based on τ rather than on τ_{ionic}. We think that this simply reflects the fact that, when at their equilibrium distance, the HCl and HBr molecules cannot accommodate an extra electron to form HCl^- and HBr^- anions with a bound electron [136–138]. For example, HCl can bind an electron to form the ground state of HCl^- only at H–Cl distances larger than 0.14 nm [137], whereas the equilibrium distance of HCl is 0.127 nm [139]. Hence the potential energy curve describing ground state HCl^- as a function of the H–Cl distance has no repulsive wall at short H–Cl distances. It consists in a shallow well close to the equilibrium distance of the HCl^- anion at 0.2 nm. The curve stops below 0.14 nm when it crosses the potential curve of neutral HCl. The consequence is that dissociative attachment to $HCl(v = 0)$ by low energy electrons does not proceed via a classic resonant structure where electronically bonded HCl^- is formed at the equilibrium distance of neutral HCl or HBr and dissociates along the inner repulsive wall of the $H + Cl^-$ potential curve [136, 140]. Instead, recent calculations show that dissociative attachment to HCl is due to non-local resonances in a superposition of 'boomerang oscillations'

reflecting short-lived wavepacket motions of the HCl^- anion and more standard resonances arising from quasi-bound states in the outer well of the HCl^- potential curve [137]. A similar picture holds for dissociative attachment to HBr [138].

Turning back to the question of time-scale in reactions (9), it becomes clear that the full electron transfer from calcium to HCl (HBr), to turn on the reaction, cannot proceed without elongation of the molecule. The dynamical factor which limits the reaction is therefore this elongation that has to be completed within the time τ, associated with the non-adiabatic transition from the covalent curve to ion-pair curve. Reactions (9) thus appear as good examples to study concertedness in harpoon reactions. Here the approach of calcium must be concerted with the elongation of the molecule to enable the electron transfer. The interpretation of the $K + CH_3I$ reaction presented in section 3.3 was grounded on a similar picture.

3.5.2. *Competition between 'Multilocation harpoon' and 'Double-harpoon' mechanisms*

Chemi-ionization is also observed as a minor channel besides reaction (8) in the $Ba + Cl_2$ collision:

$$Ba + Cl_2 \rightarrow BaCl^+ + Cl^-. \tag{11}$$

In contrast with BaCl (the product of reaction (8)), which correlated with Ba^+Cl^-, the structure of the chemi-ionization product $BaCl^+$ is close to $Ba^{2+}Cl^-$ and correlates adiabatically with the double-electron-transfer intermediate $Cl^-Ba^{2+}Cl^-$ [116, 117]. $BaCl^+$ is backscattered, suggesting that reaction (11) proceeds from a very restricted geometry with a low impact parameter and a near-collinear approach [104, 122]. This is an important dynamical difference with the competing reaction (8).

The scenario of the competition between chemi-ionization, reaction (11), and reaction (8) could be the following. It involves the 'double harpoon' mechanism originally introduced by Menzinger [116, 117]. After a first electron transfer, the newly formed Cl_2^- molecular ion is stretched rapidly as suggested in the DIPR–DIP mechanism, thus promoting reaction (8) with a high efficiency. With the language of the previous section, there is almost no dynamical limitation since Cl_2 can attach an electron without prior deformation and Cl_2^- quickly dissociates along a repulsive wall. However, for the near-collinear approach in low impact parameter collisions, momentum conservation pushes initially the nascent Ba^+Cl^- and Cl moieties together which prevents the dissociation of Cl_2^- as $Cl^- + Cl$, which otherwise would be rapid. A close-packed transient Ba^+Cl^-Cl is thus formed, which has time to transfer the second valence electron of barium. This forms $Ba^{2+}Cl^-Cl^-$. Rapid dissociation as $Ba^{2+}Cl^- + Cl^-$ follows because of the Coulomb repulsion between the two negative Cl^- ions [104, 122]. The same picture has also been proposed in $Ba + Br_2$ collisions [123]. In this case the truly limiting step in the reaction is the second electron transfer in near-collinear geometry; it can be seen as a incipient groove that is ploughed deeper and deeper at collinear geometry in the broad surface leading to $BaX + X$.

3.5.3. *Deeper insight into the 'Double harpoon' mechanism: reactions leading to divalent products*

The dynamical parameters, electron transfer distance and time-scales both for the deformation of the neutral molecule and for dissociation of the molecular anion seen in the previous sections are of importance here too. Lee and co-workers have

distinguished three classes of reactions for ground state alkaline earth atoms [115, 122, 141]:

(1) The first valence electron is transferred at long range, forming a stable molecular anion, as in the $Ba + NO_2$ reaction.
(2) The first electron transfer is still at long range, but the molecular anion can promptly dissociate, as in the $Ba + O_3 \rightarrow BaO + O_2$ reaction [122].
(3) A close collision is needed for the first electron transfer, as exemplified by the $Ba + H_2O$ reaction.

Most interesting are the first and third classes of reactions that are reviewed now.

In the reaction

$$Ba(6s^2\,{}^1S_0) + NO_2 \rightarrow BaO(X) + NO, \qquad \Delta H = -2.6\,\text{eV}, \tag{12}$$

the long-range electron transfer forms the $Ba^+NO_2^-$ electron transfer complex that does not correlate adiabatically with the ground state products BaO because of its doubly charged structure $Ba^{2+}O^{2-}$. Moreover the NO_2^- ion is stable and its dissociation as $NO + O^-$ is endoergic. Hence, for not too high collision energies, the $Ba^+NO_2^-$ complex survives for many rotational periods, without back-donation of the electron to the metal ion. This allows time for the transfer of the second valence electron of barium, which is probably hindered by an energy barrier [115, 122]. This mechanism stems from the forward–backward symmetry in the angular distribution of BaO which actually suggests that BaO decays from a long-lived collision complex. However, a direct forward mechanism, which is believed to produce vibrationally excited BaO(X), is superimposed on this dominant mechanism. An electron transfer is also conjectured to account for this channel, but in unfavourable geometries for the formation of a long-lived complex, for instance when Ba approaches very close to one of the oxygen atoms of NO_2. The reaction of barium with NO_2 also has a chemiluminescent channel, which was studied in a beam–gas arrangement. The chemiluminescence originates from $BaO(A\,{}^1\Sigma^+, A'\,{}^1\Pi)$ with a state distribution close to the prior distribution [142]. Hence, the chemiluminescent product might decay from the long-lived complex, as it is waiting for the second electron transfer.

A crossed molecular beam study of $Ba + H_2O$ collisions by Lee and co-workers has shown that BaO is the major reaction product, even at collision energies well above the barrier of endoergicity for the formation of the BaOH product. This result precludes the formation of an intermediate where barium is inserted into an OH bond. On the contrary, it was interpreted on the grounds of a concerted mechanism, with abstraction of the central O atom of HOH and simultaneous formation of H_2. This might be the result of two effects: first, a very short-distance (< 2 Å) transfer of a valence electron of barium towards the $4a_1$ orbital of water, which is antibonding with respect to both OH bonds: second, the electron jump distance is close to the bond length of ground state BaO, which has the structure $Ba^{2+}O^{2-}$. The system is therefore in good position to transfer readily the second electron required for the formation of the BaO product at the same time as the H_2 molecule is formed [115, 143].

In reaction with methanol, barium leads to the methoxide and not to BaO. This is surprising at first glance since the barium + alcohol reaction should have a similar mechanism to the barium + water reaction. In fact, the reaction starts the same with a close collision between barium and ethanol, but the concerted formation of the

H—H bond in the water mechanism has no equivalent when H—O—H (water) is replaced by H—O—CH_3 (methanol). Its equivalent indeed would be the concerted formation of H—CH_3, which should go through a three-centre TS, and would necessitate the rotation of the sp^3 carbon to put it into position for bonding with the H atom leaving OH. This is very unfavourable and the H atom prefers to migrate, hence forming temporarily the insertion intermediate $HBaOCH_3$, which decays as $BaOCH_3$+ H [143].

The above two scenarios for the reactions with water and methanol are not only supported by the nature of the reaction products; they also account for the product angular and recoil velocity distributions observed experimentally. In particular, the concerted three-centre elimination of H_2 implies a substantial bond rearrangement, which implies energy barriers in the entrance and in the exit valleys of the reaction, hence resulting into a certain duration of the collision complex, in agreement with the observed forward–backward symmetrical angular distribution of the product BaO [143]. Interestingly, these scenarios are close to those encountered in the chemiluminescent reactions of alkaline earth atoms (Ca, Sr, Ba) with stronger oxidizing agents: H_2O_2, *t*-BuOOH and HNO_3. A near-statistical distribution of the product energy states was observed, thus suggesting again that these products decay from a long-lived complex [142, 144].

3.6. *Reactions of electronically excited transition metals: 'Electron core conservation' and 'multilocation harpoon'*

Transition metals of the first row have ionization energies in the range 6.5–7.7 eV. Hence, with an additional energy of a few eV, the ionization energy of electronically excited transition metals is close to that of alkali atoms, with the consequence that reactions with oxidative molecules should proceed through a harpoon-like mechanism. An example is given by reactions of Cu with F_2 studied in the group of Parson [145, 146] and that of Sadeghi [147–151]:

$$Cu(3d^{10}4s\,^2S) + F_2 \rightarrow CuF + F, \tag{13}$$

$$Cu(3d^{9}4s^{2}\,^2D) + F_2 \rightarrow CuF + F. \tag{14}$$

The important point is the very strong increase in CuF chemiluminescence when Cu switches from the ground state (reaction (13)) to the excited state (reaction (14)). Sadeghi and co-workers pointed out that the same electron core $3d^9$ is found in excited Cu (configuration $3d^94s^2$), in the chemiluminescent CuF product that has mostly the configuration $Cu^+(3d^94s)F^-$ and in the excited ion pair $Cu^+(3d^94s)\cdots F_2^-$. Similarly, the electron core configuration $3d^{10}$ is found in ground state Cu (configuration $3d^{10}4s$), in ground state CuF (dominant configuration $Cu^+(3d^{10})F^-$) and in the ground state ion pair $Cu^+(3d^{10})\cdots F_2^-$. Assuming the conservation of the electron core $3d^9$ or $3d^{10}$ from reactants to products leads to the mechanism drawn in figure 3. Reaction of ground state Cu goes through the outer crossing with the ground state ion-pair curve leading to nonchemiluminescent reaction. In contrast, the excited Cu reaction proceeds from the inner crossing with the excited ion-pair curve, leading dominantly to chemiluminescence as observed experimentally [145, 147, 148, 151]. This is a further example of the 'multilocation harpoon' mechanism, in a situation where the core of d electrons is conserved along the reaction.

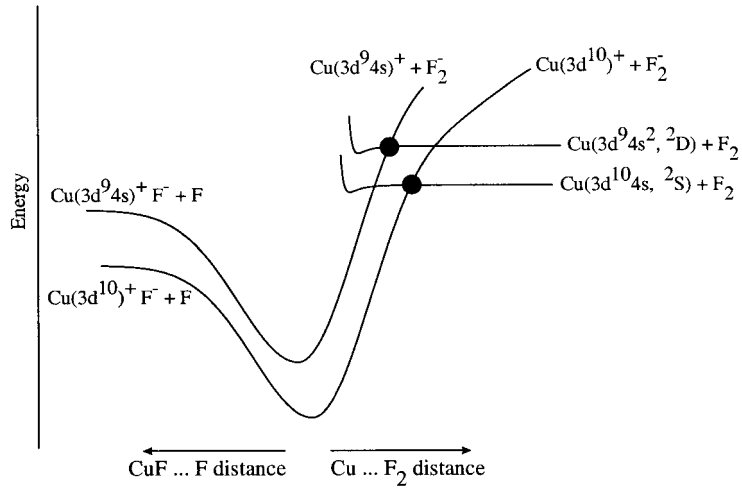

Figure 3. Potential energy diagram for the Cu + F_2 reaction. The circles indicate the crossing regions where the electron jump takes place. Adapted from [147].

Work performed by the group of Levy has addressed the question of branching to chemiluminescence in reactions of ground state and electronically excited manganese atoms with a variety of molecules [152–161].

The situation is tremendously more complicated than for the Cu + F_2 reaction because of the variety of product electronic levels that can be populated by the reaction. The general picture for these reactions is a hierarchy of covalent–ion pair crossings, with the chemiluminescent channels originating from inner crossings as in the multilocation harpoon model. The crossings are mostly at short internuclear distances, close, and sometimes within the hard sphere repulsion region of the reactants. This results in activation barriers along the reaction coordinates, a result that stems from the use of a 'multiple line-of-centre' model to analyse the data [154, 162]. In most cases, especially when the molecular partner has a small positive or a negative electron affinity, the expected barriers are so high that the reaction should involve a substantial deformation of the molecular reactant for its electron affinity to become large enough and the electron transfer to proceed. Put in other words, and considering the PESs for the reaction, the lowest energy barrier for reaction is located somewhere in the exit valley of the reaction at a configuration where the molecular reactant has been deformed enough to resemble the molecular anion. As seen several times in the present review, this leads to a dynamical constraint on the collision time, which renders the reaction unfavourable at large collision energies when the molecular reactant does not have enough time to deform. Again in the language of PESs, at large collision energies the system can no longer turn the corner in the potential surface to reach the transition state region, when it is located too far in the exit valley of the reaction.

This phenomenon appears in most manganese reactions reported by Levy and co-workers [156–161].

3.7. *'Non-harpoon' reactions of ground state transition metals*

The previous sections dealt with reactions that mostly follow the harpoon model, with a single electron transferring from the metal atom to the molecule, often at a

large separation between the atomic and the molecular reactants. The present section approaches a very different situation with reactions of ground state transition metals. The ionization energy of these metals, in the range 6–8 eV, is too large to allow for harpoon reactions even with strongly oxidative molecules such as Cl_2. The hypothetical curve-crossing distance that is calculated from the Magee formula for reaction of these metals is often deeply inside the hard sphere region of the reactants. The mechanism of these reactions follows an interpretation scheme based frontier orbital correlation with electron donation and back-donation [163, 164].

The present section surveys part of the corresponding literature for two reasons. One is because transition metals have proved over the last 20 years to be valuable centres to activate the ubiquitous but unreactive C—H bonds of saturated hydrocarbons [165]. Hence, there is a fundamental interest in understanding the interaction of transition metal atoms with molecules, no matter what they are, organic or inorganic. Work is reviewed here which endeavours to investigate the mechanisms of gas phase transition metal reactions. The second reason is that complexes formed by a transition metal atom and an organic molecule can be non-reactive in the ground electronic state and presumably could offer an interesting variety of precursors with which to approach the as yet unexplored field of TSS (see section 4 for reactions involving insertion of the metal into C—H and C—C bonds).

The recent activity on first-row transition metal reactions has concentrated on oxidation reactions: chemiluminescent reactions of Mn with O_3 [166] and Cl_2 [159]; reactions of Ti with O_2, NO and N_2O [167]; reaction of Sc with NO [168, 169]. As just said, the picture of a simple harpoon mechanisms must be abandoned for such reactions and must be replaced by electron donation and back-donation consideration. For example, the reaction mechanism proposed by Parson and co-workers, for the $Mn + O_3 \rightarrow MnO^* + O_2$ reaction, is based on a forward and backward donor–acceptor picture, with Mn approaching perpendicularly to the O_3 plane: a forward σ donation from the sd_{z^2} hybridized orbital of Mn to the $2b_1$ LUMO of O_3 is simultaneous with a π back–donation from the $4b_2$ orbital localized on the O—O moiety of O_3 to the $3d\pi$ orbital of Mn. The forward donation forms the bonding between Mn and one of the terminal O atoms, whereas the backbonding results in slackening of the $O—O_2$ bond [166].

Of course, the most attractive direction in transition metal chemistry is that towards a greater understanding of homogeneous and heterogeneous catalysis by transition metals. This has motivated a series of experimental work in the group of Weisshaar [170–176] and that of Davis [177–184] plus theoretical investigations by Siegbahn and co-workers with Weisshaar and co-workers [171, 172, 185, 186].

The reactivity of transition metals with alkenes is often described in terms of initial formation of a π complex according to the well-established Chatt–Dewar–Duncanson mechanism, a very general binding mechanism between metals and ligands [187, 188] (also that of excited ethylenic compounds). In the π complex of the metal M with ethylene, ethylene is donating electrons of the full π orbital to the s orbital of the metal. This is achieved under the σ symmetry with respect to the metal–ethylene coordinate z, with ethylene perpendicular to the z axis as $M \cdots \|$. Simultaneously, the metal M is back-donating d electrons to the empty antibonding π^* orbital of ethylene. This happens under the π symmetry with respect to the z axis. Of course, since the metal s orbital is usually not empty in the free metal, formation of the π complex necessitates the hybridization of the s and d orbitals and promotion of the s electron(s) into an empty d orbital. The electron donation from ethylene goes

therefore to a hybrid orbital of symmetry with respect to the z axis. Hence the hybridization energy implied in the s–d electron promotion and the spin-conserving or non-conserving character of the promotion appear as important factors to rationalize the reactivity of transition metals of all three rows with alkenes [170, 172, 185]. Similar considerations apply to the reactivity with alkanes [172, 178, 186].

Recent developments in this field concern the behaviour of the metal–molecule complex after the π complex has formed. Consider the elimination reaction of H_2 in the Zr + ethylene system, which has been studied both experimentally and theoretically [175, 179, 189]. The B3LYP density functional theory has been applied to characterize transition states and intermediates along the coordinate from the reactants $Zr + C_2H_4$ to the products $ZrC_2H_2 + H_2$. The reaction proceeds mostly on a triplet potential energy surface. The entrance transition state is T shaped ($Zr \cdots \|$). This enables the system to reach a first, weakly bonded π complex, which correlates with the ground state $4d^2\,5s^2$ configuration of Zr. This complex decays through a small barrier into formation of a second complex, which is a more strongly bound complex than the first one and has the structure of a metallocyclopropane compound (full electron transfer in the donation and back-donation mechanism). The latter correlates dominantly with the excited configuration $Zr(4d^3\,5s^1)$. The above-mentioned s–d promotion is at play here. The remainder of the triplet reactive surface has two wells. One corresponds to the insertion intermediate H—Zr—C_2H_3, the other to the dihydrido compound $H_2Zr \cdots C_2H_3$. The latter is connected to the exit channel by two reaction paths. One goes through a low energy multicentre transition state, corresponding to a concerted reaction process at low collision energy. The other goes through a high energy transition state, which lies 0.8 eV above the product asymptote. Besides this reaction path on a triplet potential energy surface, a second one has been conjectured which involves an intersystem crossing giving access to the singlet excited configuration of the metallocyclopropane compound. At the present stage, although quite detailed, the theoretical understanding of this reaction is not fully satisfactory because inconsistencies remain with the experimental results [189].

Reactions of Y with alkenes have also been investigated, both theoretically and experimentally. The reaction mechanism leading to H_2 elimination has a strong relationship with the preceding one with Zr; however, the question has not been completely satisfactorily answered on the theoretical side [176].

4. Transition state spectroscopy

4.1. *Probe of the TS in a full collision experiment*

Far-wing observations in chemiluminescent reactions of the type

$$A + BC \rightarrow ABC^* \rightarrow AB + C^* \tag{15}$$

were the first attempt to observe directly the TS region of a reaction [190, 191]. Wing intensities corresponding to the ABC^* emission when the system is on the way to the reaction, contain indeed direct dynamical information since they depend on the time spent by the collision pair in the ABC^* region of the PES where the wing is formed [10, 192, 193].

Far-wing observations are complemented by laser-assisted reactions where, for instance, a chemiluminescent reaction is turned on by the absorption of a photon during the collision between the reactants [194–200]. The experiment consisted in recording the chemiluminescence signal as a function of the wavelength of the laser

that promotes the reaction. Similarly, the $Mg^* + H_2 \rightarrow MgH + H$ reaction has been studied by the laser-assisted technique (pump laser), in a pump–probe scheme where the product MgH is probed by LIF [201, 202]. Reactions of excited Na have been studied by the same technique [203–205].

These experiments were very promising at the beginning, but disappointing in the long term, because of a dramatic lack of sensitivity and, more importantly, because spectra that arise from transitions between two unbound diffusion states are broad, mostly featureless and therefore difficult to interpret. Structures in laser-assisted reaction spectra only appear as satellite features, which arise from an extremum of the potential difference between the ground state and the excited.

Nevertheless, work on laser-assisted collision is continuing in the group of Kleiber [206–208], the method being fairly successful when strong alignment effects of the reactive excited orbital are to be observed. These appear as blue-wing–red-wing asymmetries in the laser-assisted reaction spectra. For example, it has been shown that π-like alignment of the 3p orbital favours the $Mg(3p\ ^1P_1) + CH_4 \rightarrow MgH + H$ reaction in a picture where the methane molecule is taken as spherical [206, 207]. In contrast, σ-like alignment is required to promote the $K(5p\ ^2P) + H_2 \rightarrow KH(v = 0, J) + H$ reaction [208]. These experiments reveal which of the excited potential surfaces correlating with the separated reactants best promotes the reaction, although the TS of the reaction is not probed directly. The absorption of the pump photon occurs indeed at large separation between the reactants, 5 Å and beyond. For this the reason satellite features observed in the laser-assisted spectrum of the $K(5p\ ^2P) + H_2 \rightarrow KH(v = 0, J) + H$ reaction could be interpreted qualitatively using the potential surfaces of Rossi and Pascale that do not include a reactive channel [209].

4.2. *Half-collisions: access to perpendicular coordinates*

The breakthrough which enabled spectroscopy of the TS region, i.e. TSS, was to stabilize reactants in a geometry close to that of the TS and to turn on the reaction by laser excitation or by photodetachment of an electron. The goal is to map movements perpendicular to the reaction coordinate as damped vibrational progressions of a dynamically constrained oscillator. The progressions are related to the transverse potential while the damping is related to the decay of the autocorrelation function of the initial wavepacket away from the transition region. The width of these transitions thus corresponds to the escape from this transition region. Three variants of this idea have been developed. They have in common the initiation of the reaction by the formation of a highly reactive species: an open shell atom or a radical. They differ by the area of the PES covered at the transition state and by the traceability of the movements as determined by Franck–Condon factors.

According to the first one, a 1:1 van der Waals complex is formed between two reactants non-reactive in their ground state PES because of endoenergeticity or the existence of a barrier at low temperatures. The reaction is turned on by laser excitation of one of the reagents. The reaction then proceeds on an electronically excited PES. In such experiments, the frequency of the laser that induces the reaction is scanned while the reaction products are monitored. This provides the so-called action spectrum of the reaction. It is a spectroscopy of the reacting system in the TS region of the reaction, assuming that the geometry of the ground state van der Waals complex prepares the system close to the Franck–Condon region that enables excitation in the TS region [210, 211]. The typical separation between the reagents

in the van der Waals complex is 3–4 Å. Hence, this selects out reactions occurring at 'long' distances, i.e. those involving charge transfer processes.

The second approach is still to form a 1:1 complex. Here, the photodissociation of a molecule within the complex prepares a radical. This radical reacts in a pre-aligned geometry and in a range of translational energies determined by the dissociating photon. The important point is that the reaction is initiated from a known geometry, thus documenting the stereodynamics aspects of the TS region. This approach was pioneered by the group of Wittig [212, 213].

Finally, the electron photodetachment in negative ions as performed by the group of Neumark is in the same spirit as the first van der Waals experiments [214–217]. This technique gives direct access to the TS of the reaction in reactions occurring at shorter distances, as determined by the negative ion geometry that can be quite strongly bound. It allows the spectroscopy of TSs of ground state reactions to be performed. Importantly, the ground state surface of many systems can be documented here; the only limitation is the existence of a positive electron affinity for the initial pair, which might not be the case for many metal–molecule pairs. This approach offers a case example of perpendicular vibrations, as observed on a model system Br–H–I^-. There, dynamics constrains the system to vibrate along a quasi-periodic orbit after the photodetachment. In figure 4 the surface is represented along mass-weighted coordinates; the antisymmetric vibration ν_3 involves the H atom movement and is observed in the photodetachment spectra scanning through the transition state as seen on the figure. It is quasi-bound, being perpendicular to the potential of the dissociation channel (loss of an iodine atom)as represented in figure 4.

In turn TSS experiments on ground state reactions in cationic states have not been performed for bimolecular reactions, despite the interesting experiment of Bondybey on the photodissociation of CH_3I^+ [219]. This experiment can, however, be viewed as a mapping of the neutral photodissociation exploration of the CH_3I^+ ion at distances far from equilibrium in a Raman process. There are probably few reasons other than experimental for this lack of experiments; one could be the existence of deep wells in the entrance valley trapping the reactants for a long time before reaction.

Last but not least, the other advantage of these body-fixed TSS experiments is to have allowed time domain experiments in bimolecular reactions since bimolecular

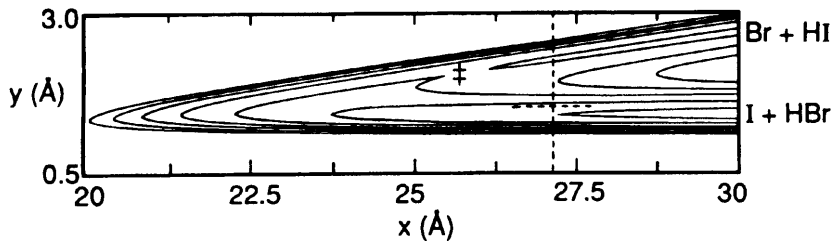

Figure 4. Potential energy surface along mass-weighted coordinates of the I + HBr reaction. Here $x = [(\mu_{\text{I–HBr}}/\mu_{\text{HBr}})^{1/2} \times (R_{\text{I}} - R_{\text{cm(HBr)}})] \sim 7.0 R_{\text{I–Br}}$, $y = R_{\text{HBr}} R_{\text{I}}$ and R_{cm}(HBr) are the position of the I atom and the centre of mass of HBr, $\mu_{\text{I–HBr}}$ is the reduced mass of the I,HBr system. The skew angle is given by $\tan\theta = [m_{\text{H}}(m_{\text{H}} + m_{\text{I}} + m_{\text{Br}})/m_{\text{Br}} m_{\text{I}})^{1/2} \sim 8^\circ$. Contours are plotted at 0.161, 0.461, 0.761, 1.061, 1.361, 1.661 and 1.961 eV with respect to the I + HBr asymptote. From [218].

complexes fix the reagents in the same geometry at the origin of time (see details in section 6).

4.3. *Probing the TS region in oxidation reactions of Ca and Hg atoms*

The present section reviews studies on reactions of electronically excited metals, Hg and Ca, which are performed by time-independent spectroscopy in a 1:1 van der Waals complex. This documents movements in the reactive system that are perpendicular to the reaction coordinate.

One could think that the models introduced earlier in this review, namely the double-harpoon and the DIPR–DIP models, are oversimplified. Instead, the present section confirms their simplicity and predictivity in explaining the branching of excited state metal reactions to luminescent products.

Section 3.4 has emphasized the role of the relative orientation of the reactants: geometrical orientation or orbital orientation of an electronically excited metal with respect to the relative velocity vector of the reaction. This applies to excited metal orbitals with p or d symmetry and has been called polarization effects previously, where in the laboratory frame the polarization of the light aligns the excited orbital. Instead, reactions initiated within the molecular 'body-fixed frame', within a van der Waals complex formed by the reagents, offer a powerful way to study this problem of the relative orientation of the excited orbital of the metal, directly in the frame of the reactants. When an electron transfer reaction is light initiated in the complex, the relative orientation of the orbital with the approach coordinate of the reagents is dictated by the orbital symmetry of the accessed state and in this electronic state the reagents have a fixed, specific, orientation. The resulting bimolecular excited state reactions promoted by optical excitation of a van der Waals complex formed by the reactants are accessed directly via the excited reaction complex. This allows for the direct spectroscopic investigation of the reaction surface in the excited state, through the laser-induced spectra of the reaction. This was first shown by Jouvet *et al.* [210, 220, 221]. (The reactions within van der Waals, complexes are also closely related to laser-assisted collisions, as developed for chemical reactions by Setser (223–225], where the reaction complex is attained from the dissociative collision pair in the ground state complex instead of the bottom of the potential well of the interaction van der Waals potential. In a scheme later called laser photoassociation [226], the colliding ground state collision pair is transferred into the quasi-bound potential domain of the reacting excited complex. The studied systems involve harpoon-type reactions in xenon-halogenated compounds. In this manner, laser-assisted reactions have been performed in low pressure gas mixtures of Xe with Br_2, CCl_4, CCl_3Br, and I_2. The products are XeCl(B, C), XeBr(B, C) and XeI(B, C) following two-photon promotion to the reactive ion-pair potentials. The utilization of a two-colour scheme emnhances the two-photon, laser-assisted reactions because of a better match with an intermediate state of the reagent molecule. In this work interesting preferences in the reactions with mixed halogenated compounds have been found in the final excited state products.) The resulting spectra are called action spectra. The explored region in the reaction on the reaction surface depends on the Franck–Condon allowed window from the ground state. The reaction initiated in van der Waals complexes explores ideally excited state harpoon reactions. The latter occur at intermolecular distances in the range 3–10 Å, a region which is Franck–Condon accessible from ground state van der Waals complexes, whose equilibrium distances are typically R = 3–4 Å.

4.3.1. *Local excitation and subsequent electron transfer*

4.3.1.1. *Excited mercury chemiluminescent reactions.* The first example of such reactions is the reaction of excited mercury, $Hg(6s6p\,^3P_1) + Cl_2$ [210] in which the crossing seam of the neutral and ionic (correlating with $Hg(6s\,^2S) + Cl_2^-$) surfaces, can be directly observed, with the precision of tunable laser excitation. The excited mercury atom becomes open shell with an ionization energy close to 5 eV, similar to a sodium atom, and the resulting ionic covalent crossing occurs at 4 Å. A schematic of the reaction and observation conditions is shown in figure 5, where the reaction has sufficient energy to produce excited state products $HgCl(B\,^2\Sigma^+)$, with an excess energy of 0.8 eV. A laser scans the potential energy surface of the excited state reaction and yields the chemiluminescent product HgCl observed via the B–X emission. The resulting action spectrum appears in figure 6, where a broad continuum of 1000 cm^{-1} width is followed by a peak and falls abruptly, 400 cm^{-1} after the mercury line. This spectrum indicates without ambiguity that the transition accessed by the laser relates to the local excitation of the mercury, exciting a surface that joins the neutral asymptote $Hg(6s6p\,^3P_1) + Cl_2$. Above this asymptote, if a reactive state were accessed, it would easily compete, owing to a high gradient to the products, against the dissociation into $Hg(6s6p\,^3P_1) + Cl_2$ with only a small gradient to the fragments. The specific shape of the action spectrum shown in figure 6 reflects the nature of the upper excited surface as excited from the fixed bimolecular complex. The geometry of this ground state complex is presumably T shaped with the mercury in contact of the chlorine molecule with the minimum repulsion; the excited $Hg(6s6p),^3P_1$ complex should be the same and two electronic states of the complex will be created depending on the orientation of the Hg(6s6p) orbital with the Hg–Cl_2 molecular axis.

The presence of chlorine induces a strong ionic covalent mixing, *c.* 1 eV [227]; this causes the Hg 6p orbital to be decoupled from the 6s orbital. In this instance, in a triatomic T-shaped molecule, there will be several states depending on the orienta-

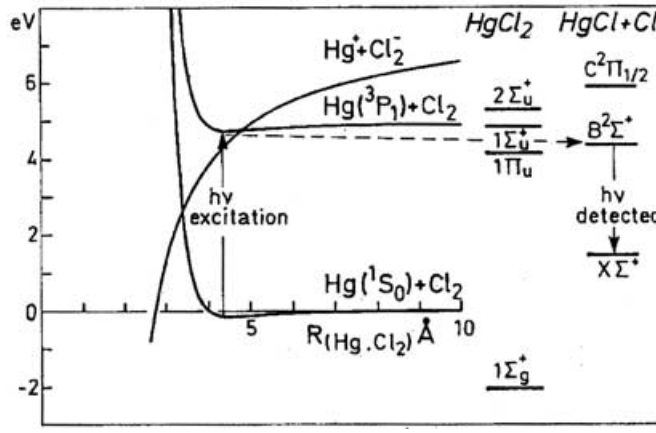

Figure 5. Potential energy diagram of the reaction of Hg with Cl_2 along the $R_{Hg–Cl_2}$ coordinate. The excitation Franck–Condon region is reproduced and the position energy levels of the HgCl product are drawn to scale, together with the insertion product ClHgCl levels. The latter product is not observed, since it cannot be energetically chemiluminescent. Adapted from [210].

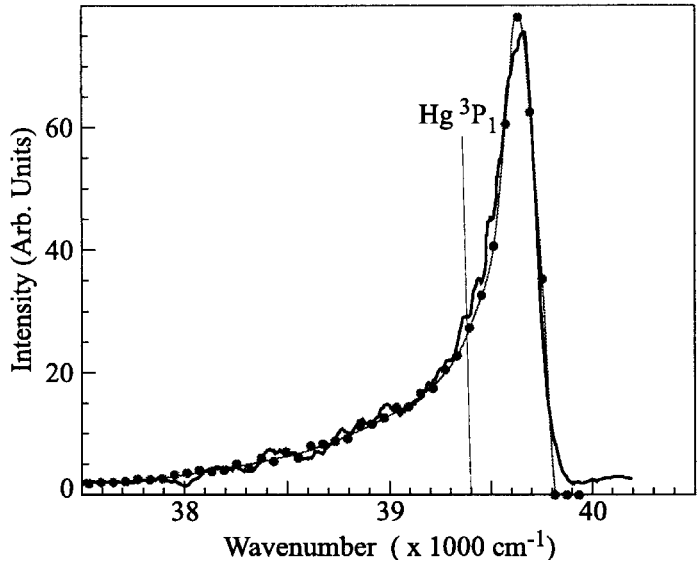

Figure 6. Full curve, action spectrum monitoring the HgCl emission, while scanning the laser inducing the reaction in the region of the Hg resonance line. The spectrum is broad and falls off sharply 400 cm^{-1} after this line. Dots: simulation by the model operating over the coordinates R_{Hg-Cl_2} and θ_{Hg-Cl_2} on the surface described below and in figure 7.

tion of the Hg 6p orbital with respect to the molecular plane: two A″ states with an in-plane 6p orbital and one A″ state with the the Hg 6p orbital perpendicular to the $Hg\cdots Cl_2$ plane. This A″ state has for symmetry reasons no direct coupling element with the ionic reactive state $Hg(6s\,^2S) + Cl_2^-$, since it has a zero overlap with the antibonding orbital of the chlorine molecule. As a first step, we shall not consider it. We thus remain with the two A″ states with the in-plane 6p orbital that we label as Σ and Π, corresponding to 6pσ and 6pπ orientations with respect to the Hg–Cl_2 axis, in a quasi-diatomic approximation. Hence, the action spectrum is interpreted in the following way: the state accessed by the excitation laser has a compound character, covalent, $Hg(6s6p)^3P_1\cdots Cl_2$, and ionic $Hg(6s)^+$—Cl_2^-. These states are mixed and the mixing drives the reaction. After excitation in the Franck–Condon window opened by the geometry of the ground state $Hg\cdots Cl_2$ complex, the system is launched on the upper reactive surface. All the excited complexes will have reacted and formed either the ground (not detected) or the excited state of HgCl. The question is now, how to build a reactive surface correlating with the excited state of mercury $Hg(6s6p\,^3P_1)$ in the absence of calculations on this system.

The Π state of this surface should be very attractive and benefit from the full ionic covalent mixing coefficient; then it would appear displaced at lower frequencies by presumably 1 eV from the mercury line, which has not been observed. In turn the Σ covalent state has no coupling element to the ionic state in C_{2v} geometry since the Hg(6p)σ orbital has a cancelling overlap with the π_u antibonding orbital on Cl_2^- (figure 7, panel 2). Hence the coupling of the covalent Σ state surface with the charge transfer $Hg(6s)^+$—Cl_2^- surface is a typical example of a conical intersection between the covalent T-shaped surface and the ionic surface leading to the product Cl + HgCl(B).

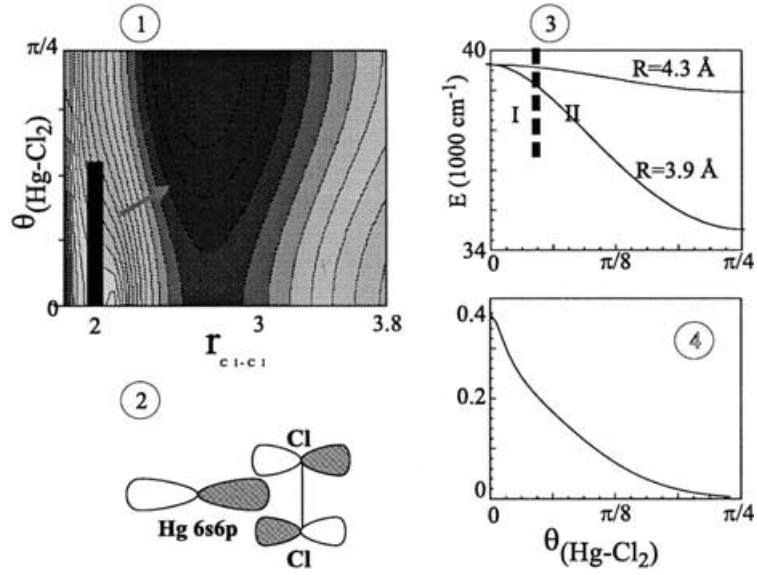

Figure 7. Panel 1: reactive surface built along the $r_{Cl–Cl}$ coordinate and the angular coordinate $\theta_{Hg–Cl_2}$. The Franck–Condon window is represented at $r_{Cl–Cl} = 1.988$ Å. Panel 2: scheme of the C_{2v} configuration in the Σ state for Hg(6s6p)$\cdots$Cl—Cl. Panel 3: cut of the angular potential at the Franck–Condon window for two values of $R_{Hg–Cl_2}$, upper 4.3 Å, lower 3.9 Å. Panel 4: excitation function of this surface represented as a function of $r_{Cl–Cl}$ for $R_{Hg–Cl_2} = 3.9$ Å; $\psi(R,r,\theta)^2 a^2_{\text{ionic–covalent}}$ where $a = \sin(\phi/2)$ and $\tan(\phi) = 4H_{IC}/(E_I - E_C)$.

The excited PES is constructed from the covalent excited potential due to the interaction of the Hg(6p)σ orbital with chlorine, V_C, and the ionic potential resulting from the Hg(6p)σ electron transfer to chlorine, V_I. These PESs are represented in Jacobi coordinates: $r = r_{Cl–Cl}$, $R = R_{Hg–Cl_2}$ and $\theta = \theta_{Hg–Cl_2} - \pi/2$. The variation along r corresponds to the Cl–Cl stretch, R to the van der Waals interaction or ionic interaction between mercury and Cl_2 or Cl_2^- and θ to the Hg$\cdots$$Cl_2$ chlorine bending motion with a barrier to linearity. The covalent potential is thus expressed as

$$V_C(R,r,\theta) = V_{\text{Morse } Cl_2}(r) + V_{\text{Morse, van der Waals}}(R) + V_{\text{van der Waals}}(\theta). \tag{16}$$

Numerically it is

$$V_C(R,r,\theta) = 20\,000\,\{1 - \exp[-2.05(r - 1.988)]\}^2 + 100\,\{1 - \exp[-2.05(R - 4.8)]\}^2 - 100 + 50\,(1 - \cos\theta). \tag{17}$$

Similarly, the ionic potential is given by

$$V_I(R,r,\theta) = I_p(\text{Hg}) - \text{EA}(Cl_2) + V_{\text{Coulomb}}(R) + V_{\text{charge–quadrupole}} + V_{\text{Morse } Cl_2^-}(r), \tag{18}$$

$$V_I(R,r,\theta) = 64\,903 - \frac{116\,150}{R} - \frac{1.25 \times 10^6}{R^4} + 10\,162\,\{1 - \exp[-1.21(R - 2.7)]\}^2. \tag{19}$$

In the numerical expressions, the distances are given in angströms and the energies in wavenumbers. The covalent and ionic surfaces are coupled with an angle-dependent matrix element $H_{IC}(R,\theta) = 8065 \sin(2\theta) \exp(R - R_C)$. The coupling is zero at the T-shaped geometry $\theta = 0$ and at the linear geometry $\theta = \pi/2$. It has an exponentially decreasing extension after the ionic covalent crossing distance R_C. The resulting surface is split in two lobes connected at $\theta = 0$ by a conical intersection. It is calculated by two-state perturbation in the standard form:

$$V_e(R,r,\theta) = \frac{V_I(r,R) + V_C(R,r,\theta)}{2} \pm \frac{\{[V_I(r,R) - V_C(R,r,\theta)]^2 + 4H_{IC}(R,\theta)^2\}^{1/2}}{2}. \tag{20}$$

Here, the relevant surface corresponds to the minus sign in the above equation. The ground state surface is represented by a Morse potential with a 400 cm^{-1} depth and a 100 cm^{-1} barrier to free rotation. The spectrum has been simulated at the equilibrium distance of chlorine $r = 1.988$ Å. The potential difference between the excited $V_e(R, r = 1.988, \theta)$ and ground $V_i(R, r = 1.988, \theta)$ surfaces was developed on a 50×50 grid. An excitation function was assigned to each point of the grid. This function $EF(R,\theta)$ is the product of two terms: the first is the ground state probability function at this point of the grid determined by $\psi(R,r,\theta)^2$. If it is assumed that the electronic excitation results from the covalent component of this surface, the second term a^2 represents the weight of the covalent component at these coordinates R,θ of this point on the excited surface. This covalent term a^2 is simply obtained from perturbation theory, where $\tan(\phi) = 4H_{IC}/(V_I - V_C)$ and $a = \sin(\phi/2)$. All contributions are summed in bins at fixed frequency intervals and compared with the experimental spectrum.

The experimental curve is well fitted by the simulation; figure 6. The determining factor is the extension of the ground state angular wavefunction. The shape of the experimental spectrum, a peak at 39 500 cm^{-1} and a broad tail beyond, reflects the angle–dependent shape of resulting upper surface, as shown by a cut along the angle θ at the vertical of the ground state of the complex (see panel 3 in figure 7). Close to $\theta = 0$ the potential is flat and mostly covalent producing the peak (region I), while at larger θ the gradient becomes strong (region II) and generates the broad trailing continuum.

Actually, the previously mentioned, but neglected, A″ alignment of the Hg 6p orbital could have a contribution, underlying the simulated spectrum in region I. It would correspond to the excitation of the $HgCl_2$ A″ van der Waals potential, only indirectly perturbed by the ionic reaction surface.

As a difference from earlier publications [221], where essentially a small ionic covalent coupling was used in the simple harpoon model (only on the Hg–Cl_2 coordinate was considered), the angular dependence of the upper potential is essential in reproducing the experimental data. In fact the earlier simulation averaged the coupling over all accessible angles on the surface and did not reproduce fully the experimental data. The Franck–Condon excitation of the ground state Hg–Cl_2 allows here an investigation of a relatively broad region of the TS region in the excited state reaction of $Hg(6s6p\,^3P_1) + Cl_2$ reaction in perpendicular geometry. This region extends from the mainly covalent domain, in region I of figure 7 panel 3, to the mainly ionic domain, region II.

It must be mentioned that region II is still relevant to the TS since we have not introduced the formation of the Hg—Cl bond. It must be mentioned that the agreement between simulation and experimental spectra is extremely robust in terms of the parameters used for the simulation yields. Hence $HgCl_2$ appears as an excellent example of the multidimensional character of the TS region.

This example has not taken into account the correlations with excited ionic surfaces accessed by 6s electron transfer because these surfaces lie at too high an energy in the case of mercury. This type of electron transfer will be described in the following section.

4.3.1.2. *Ca-HX excited state reactions.* The reaction of excited state calcium with hydrogen chloride had been considered by Bernstein *et al.* [228] as a case example where excited state body-fixed orientation could be achieved, in relation to the polarization, collision experiments of Rettner and Zare [103]. The reactions of locally excited calcium, in $4s4p\,^1P_1$ and $4s3d\,^1D_2$ states, complexed to the hydrogen halides HF, HCl, HBr and HI have been observed within the body frame of the excited van der Waals complex, while the excited state reaction products were detected [229–231] by luminescence or the ground state products were detected by laser induced fluorescence (in the case of Ca–HCl) [232]. Also, full collision experiments conducted by the group of Gonzàles-Ureña [111, 233] have yielded interesting comparisons. In the full and half-collisions of excited Ca with HX, the open decay channels are

- $Ca^{**} + HX \rightarrow Ca^{*} + HX$—electronic relaxation of Ca, where Ca^{**} stands for the $4s4p\,^1P_1$ and $4s3d\,^1D_2$ states and Ca^{*} one of the lower calcium states,
- $Ca^{**} + HX \rightarrow CaX + H$—ground state product formation,
- $Ca^{**} + HX \rightarrow CaX(A, B) + H$—excited states product formation.

The ground and excited states A, B of the CaX product are observed to be the essential outcomes of the half-collision, which electronic relaxation does not seem to be able to compete with. Detecting excited or ground state products yields quite expectedly different results.

4.3.1.3. *Local excitation of the metal.* Here we encounter a new situation. The local excitation of the calcium chromophore from the ground state $Ca\cdots HCl$ complexes transfers the complex in a strongly attractive van der Waals potential amidst two electron transfer regions: the transfer of the 4p or 3d electron at long $R_{Ca–HX}$ distances to form $Ca^+(^2S)$—HX^- and, at short distances, the transfer of the 4s electron to the excited $Ca^+(^2D)$—HX^-. Both crossings will differ from one halogen to the other owing to the variation in the electron affinity of HX (negative for free HF to positive for HI) and will also vary with the locally excited region in Ca* of the potential. This will condition the dynamics of the excited state reaction and its branching to excited state products among which the Ca–HBr system is the most efficient.

To investigate excited state potentials of these complexes, in the same manner as for Hg—Cl_2, action spectra have been recorded detecting the $A\,^2\Pi$ and $B\,^2\Sigma$ states of CaX. These spectra are remarkably similar in appearance from $Ca\cdots HF$ through Ca—HI. What is striking, different from the former example Hg—Cl_2, is the presence of extended structures corresponding to vibrational progressions in the spectra, as seen in figure 8.

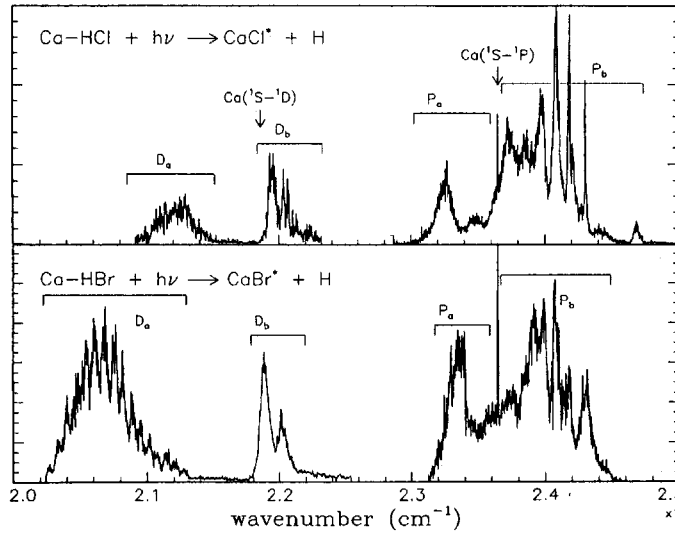

Figure 8. Action spectra recording the CaX($A\,^2\Pi$) emission while scanning the laser inducing the excited state reaction for X = Cl (top) and X = Br (bottom). The van der Waals precursor has been created in a supersonic beam resulting from the expansion of argon containing HX and laser-ablated calcium. One notes the great similarity of the spectra extending from 20 000 cm^{-1} (500 nm) to 25 000 cm^{-1} (400 nm) and the prominence of vibrational structure. The $4s^2\,^1S_0$–$4s4p\,^1P_1$ calcium line arising from collisions is indicated as a reference while the $4s^2\,^1S_0$–$4s3d\,^1D_2$ line is not observed but marked; therefore the bands are labelled according to the locally induced transition P or D after the neighbouring calcium line. Adapted from [229].

The spectra indicate that the excitation is local, corresponding to the promotion of a 4s calcium electron to a 4p or 3d orbital. This stems from the general appearance of the action spectra with two regions on the side of each atomic transition $Ca\,^1P_1 \leftarrow Ca\,^1S_0$ or $Ca\,^1D_2 \leftarrow Ca\,^1S_0$. The spectral distribution of these transitions is similar to the equivalent transitions of non-reacting van der Waals complexes with metal chromophores. The spectral distributions and the vibrational progressions have been interpreted with model potentials. This interpretation was confirmed by the calculations of Dubernet and Hutson on the open shell van der Waals complexes Ca–HX correlating with $Ca\,^1P_1$ [234]. They found that the electrostatic interaction between the excited Ca (quadrupole) and HX (dipole) yields the following potentials, which are labelled according to the C_2 symmetry group:

- Two states have A′ symmetry, one with a linear equilibrium geometry similar to the one expected for the ground state of the complex and another one with an in-plane 4p calcium orbital. The two potentials exhibit avoided crossing and states in separate energy domains result: the low energy linear complex with $p\sigma$ configuration and a high energy non-linear one with an in-plane 4p orbital.
- Another has A″ symmetry with a T-shaped equilibrium geometry and an out-of-plane 4p orbital.

In the action spectra the states have been well identified. The first A′ transition corresponds to the $4p\sigma$ linear complex observed in the red of the spectrum with respect to the atomic line (labelled P_a in figure 8) and the A″ excited T-shaped complex follows with an extended vibrational progression (labelled P_b in figure 8).

On the blue side of the P_b bands, the remaining transition A' can be found in the case of Ca–HCl at 24 700 cm^{-1}, as a broad, distinct, weak structure. From the ground state geometry of the complex with a linear $Ca \cdots HX$ structure, the general features of the observed spectra are reproduced in the model of local excitation: a similar red-shifted line to the $Ca\ ^1P_1$ line corresponding to the $A' \rightarrow A'$ absorption within the complex and blue-shifted absorption with intense bending transitions corresponding to a 90° geometry change in the $A' \rightarrow A'$ transition.

The same line of argument can be invoked for the ^1D domain in terms of the local excitation of the calcium. The observation of two domains, D_a and D_b, is clear for all the complexes except for Ca–HF where only the blue-shifted domain D_b is apparent in the action spectra. The observation of the atomic forbidden transition $4s3d\ ^1D_2 \rightarrow 4s^2\ ^1S_0$, within the complex, has been interpreted for HCl, HBr and HI [231, 235] as a lifting of the S–D forbidden character in the complex, through mixing with the nearby $^1P_1$ states of A' and A'' symmetry.

As an example, the dynamics of the reacting complexes in the A'' state (T-shaped complex with the $4p\pi$ orbital out of the plane) is well described by wavepacket calculations. The experimental result is recalled in the left-hand panel of figure 9 (top curve), where only the group of bands located on the blue side of the calcium line, which were labelled as P_b in figure 8, are relevant to the A'' excitation. A two-dimensional potential has been used for the Ca–HBr complex to model the evolution of the hydrogen motion for a fixed Ca–Br distance. The surface is constructed from the bending Ca–HBr van der Waals potential [230] and the Morse potential representing HBr. The reaction on the surface corresponds to the H atom passing

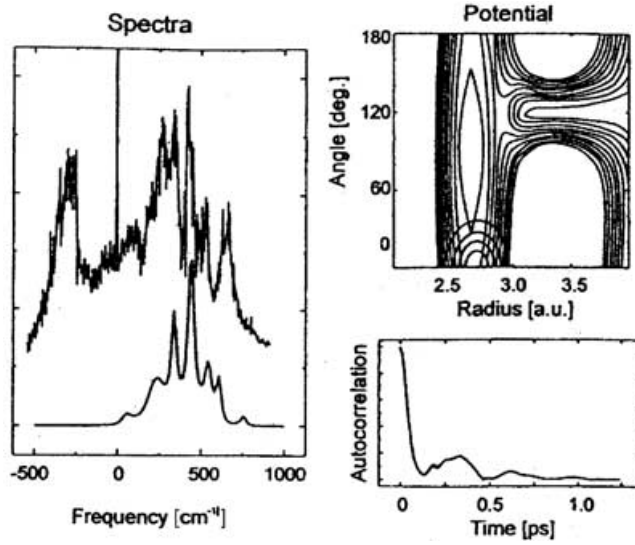

Figure 9. Result of the two-dimensional calculation for Ca–HBr. The calculation and the spectrum of the $P_b(A' \leftarrow A'')$ transition are compared at the left of the figure. The two-dimensional surface built on the reaction coordinate R_{HX} and the Ca–HX bending angle is displayed in the top right-hand panel. The propagation was performed over 1.25 ps. Each contour corresponds to 500 cm^{-1}. The contour of the Gaussian wavepacket issued from the ground state by vertical excitation is also shown in this surface. The bottom panel at the right shows the resulting modulus of the autocorrelation function with clear recurrences. Adapted from reference [229].

the transition state, which is a narrow channel at a 120° bent configuration of the Ca–H–Br molecule (see the upper right-hand panel of figure 9). The reactive trajectories initiated from the Franck–Condon region represented at 0° in the same panel can find this channel either directly or after one or several oscillations. Quantal calculations of the reactive flux are made numerically by wavepacket propagation [216, 218]. This is the quantal analogue to classical trajectories. The probability of returning close to the origin is given by the autocorrelation function shown in the bottom right-hand panel of figure 9. The Fourier transform of this function simulates the action spectrum of the reaction. The result of this simulation is shown as the bottom curve in the left-hand panel of the figure. The potential surface shown in the figures, and more specifically the position and width of the funnel, was adjusted for the simulation to reproduce the positions and width of the experimental action spectrum [229]. It must be mentioned that the fit is not very sensitive to the bending angle, but the essential conclusion is that the transition state is far from linear.

The picture of the reaction is that of the Ca···HBr complex having bending oscillations on either side of the channel where it reacts with high efficiency. Outside this geometry no reaction occurs. This is a one-potential picture whereas two potential surfaces are expected in harpoon reactions: a covalent surface and an ion-pair one. This is due to the locally high efficiency of the coupling between both surfaces at the bent configuration of Ca—H—Br. Presumably, this can be due, at least partly, to an optimum overlap between the diffuse antibonding orbital (LUMO) of HBr, mainly localized on the hydrogen, and the 4s orbital of calcium at non-linear geometries of the Ca—HBr complex. In the same manner, the action spectrum for the reaction in the Ca···HI complex is broad and almost featureless, corresponding to an even broader intersection between the ion-pair and covalent surfaces.

In contrast, this single-surface model does not apply to Ca—HCl, and a two-surface calculation was performed where the H atom movement is induced by the electron jump from the van der Waals potential to the electron transfer potential. The quantal nature of this non-adiabatic transition allows all the features of the spectrum to be reproduced. This includes the small linewidth of some transitions and, more importantly, the inverse energy dependence observed in the spectrum, where the broadest bands are those of lowest energy [230].

Lastly, the action spectra in Ca–HF close to the energy threshold to chemiluminescence display very narrow lines indicating the partial closure of the corresponding reactive excited state channel. This indicates that the observed channel luminescence is independent of the ground state channel that could also contribute to the broadening of the lines in the spectrum and confirms the model of the 4s electron hop, separated from the 3d one. We shall now examine the effect of this hop on the efficiency of production of excited states.

4.3.1.4. *Mechanism of production of excited states: excited ionic curves.* The mechanism for the production of excited states has been already invoked in the case of excited state barium reactions. It has also been discussed by Zare and co-workers when investigating polarization effects in the chemiluminescent reaction of aligned $Ca(4s4p\,^1P_1) + HCl$ and other halogenated molecules [102, 103]. Following their analysis, the excited states of the calcium products correlate directly with an excited ionic electron transfer potential: here the lowest is the $Ca(3d\,^2D)^+ + HX^-$ potential. The reaction results from the crossing of the locally excited potential

correlating with $Ca^* + HX$ with this excited ionic potential $Ca(3d\,^2D)^+ + HX^-$. Specifically it is shown that the crossing is possible within the range 3–5 Å of the excited van der Waals potential [231]. Symmetry effects result, termed core symmetry conservation, where the excitation of a specific excited state of the complex (of a given orbital symmetry) yields CaX products in the equivalent symmetry. A″ and A′ states of the Ca—HX complex yield preferentially states of CaX with respectively Π and Σ symmetries. This corresponds to the covalent–ion pair crossing where the 4s electron of the calcium has transferred to HX leaving the Ca core with the initial symmetry. In figure 10 an example is given of this preferred core conservation where the A″ symmetry excited Ca—HBr complexes form preferentially the CaBr $A\,^2\Pi$ state and conversely A′ states of the complex will populate the CaBr $B\,^2\Sigma$ state, despite unfavourable energetics: the lowest energy state of the product should always be the most populated. The flux to the CaBr $A\,^2\Pi$ state, although being modulated by the excitation in either the P_a (A′) or the P_b(A″) transitions, is always important. The reason for the lesser correlation of the A′ excited state of the Ca···HBr complex with CaBr($B\,^2\Sigma^+$) emission may be found in the outer electron transfer, at the crossing of the ground state ionic curve and the locally excited state. Reactive trajectories passing through this crossing are not expected to yield chemiluminescence, but ground state CaBr instead. Here, in the A′ symmetry with the Ca 4p orbital pointing towards HCl in σ symmetry, the electron transfer will trap states of core symmetry and divert them from chemiluminescence. The flux to BΣ states will be decreased accordingly.

As outlined above, the mechanism for channelling reactive flux into the chemiluminescent channels via the inner crossing with the excited ionic potential well accounts for the effect of preferential population of CaCl($A\,^2\Pi$) observed in the

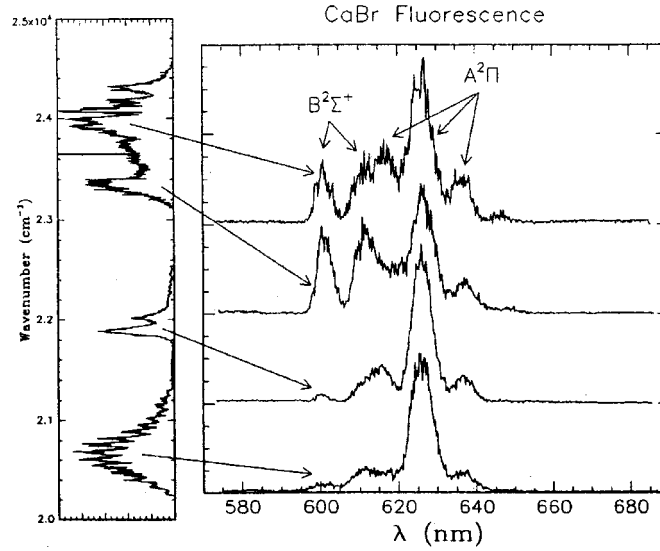

Figure 10. Chemiluminescence spectra of CaBr following different excitations of the Ca···HBr complex, as indicated by arrows connecting the excitation region on the action spectrum (displayed vertically on the left of the figure) to the corresponding chemiluminescence spectrum (shown horizontally). From top to bottom P_b, P_a the ratios, from simulations, are $(A/B)_{P_b} = 2$ and $(A/B)_{P_a} = 1.1$ respectively. Next come D_b and D_a whose ratios are 11 and 5. Adapted from [231].

full collision experiment $Ca(4s4p\pi) + HCl$ performed in the group of Zare [103]. This is supported further by elegant experiments performed by the group of Gonzalez-Urẽna on full collisions of $4s3d\,^1D_2$ metastable calcium atoms with HX molecules (X = Cl, Br) at various translational energies. The production of chemiluminescent species CaX in the $A\,^2\Pi$ or $B\,^2\Sigma$ states shows a clear threshold at 280 meV for HCl [230] and 215 meV for HBr [237]. This threshold has been modelled by De-Castro-Vittores *et al.* [238] as a barrier due to the crossing with the excited ionic potential correlating with the excited ion $Ca(3d,{}^2D)^+$. This crossing 2 in figure 11, results in the 4s electron transfer to HX thus forming an excited ionic complex. In order to access this inner crossing the system has to pass crossing 1 that mixes the $Ca(4s3d\,^1D_2) + HX$ and $Ca(4s4p\,^1P_1) + HX$ covalent

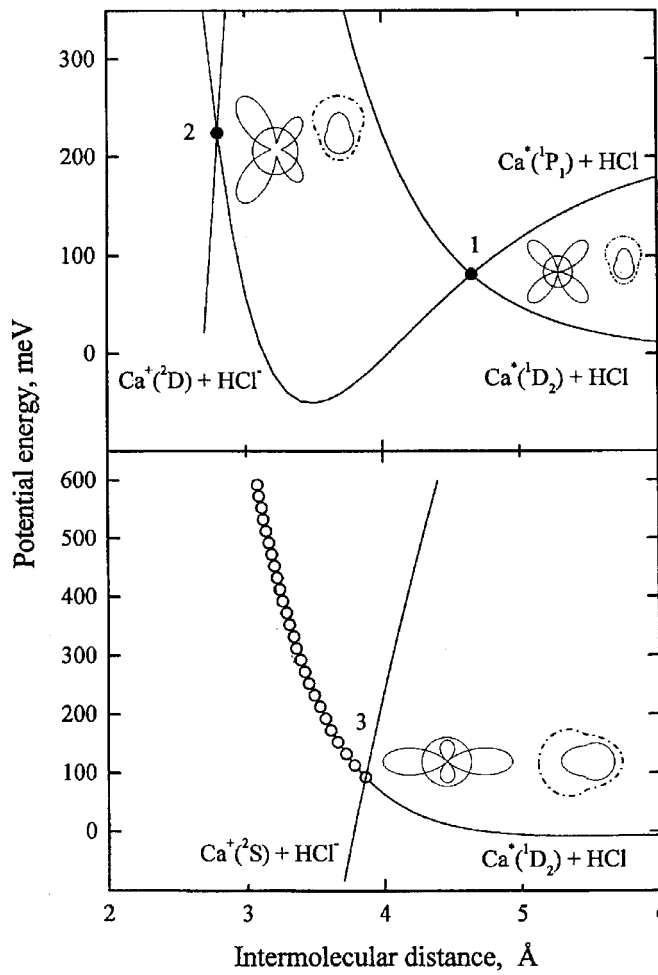

Figure 11. Schematics of the one-dimensional interaction potentials between Ca and HX in the vicinity of the $^1P_1$ and $^1D_2$ states of calcium. The crossings with the ground state ^2S and ^2D electron transfer potentials are indicated by points 1, 2 and 3. Also represented is the most favourable electronic configuration of the calcium for this transition. Adapted from reference [238].

potentials. The coupling is, as we have seen, important and therefore the process efficient. This mechanism proposed by Rettner Zare [103] finds here a quantitative confirmation. In turn the formation of the ground state products directly proceeds at the outer crossing 3 with the ground state ion curve by Ca 4p electron transfer to HX.

4.3.1.5. *Quasi-direct excitation of the electron transfer potential surface in the Ca—HCl complex.* The other important channel in the decay of the Ca—HX complex, the ground state of the product CaCl, can be observed by laser-induced fluorescence and a very high vibrational excitation is detected. This high vibrational excitation arises from the sudden release at 4 Å of the ground state CaCl molecule, thereby in a highly excited vibrational state; the distribution, maximum at $v = 30$, extends to $v = 60$. The resultant energy distribution has been interpreted with the use of the DIPR–DIP model [232].

When the high vibrational levels of the ground state of CaCl are monitored, the action spectra appear strikingly different from the preceding structured spectra, while the chemiluminescence is detected. In the case of excited product detection the action spectra are assigned to local electronic excitation of the calcium within the Ca—HCl complex, resulting in states of A′ or A″ electronic symmetry correlating with the optically accessible calcium states $4s4p\,^1P$ or $4s3d\,^1D$, within the complex. On the other hand the continuous action spectrum exhibiting a Gaussian shape while ground state CaCl is being detected is assigned here to an excitation of a different nature, i.e. the direct excitation of the charge transfer surface Ca^+HCl^- with A′ symmetry correlating with the $Ca^+\,^2S_0$ ground state ion. The excitation region corresponds to a fairly steep potential surface, the lowest charge transfer potential surface $Ca^+(4s\,^2S)$–HCl^-, that correlates with the ground state products $CaCl(X) + H$. Vertical excitation of this surface from the ground state of the Ca—HCl complex is possible owing to its partial ionic character [239]. The transition intensity can be represented by excitation to a Coulomb potential along the coordinate, R_{Ca-HCl}, with the equilibrium distance of the ground state complex as 3.8 Å and the width of the potential as 0.5 Å. With this simulation there is a reasonable agreement, given the simplicity of the model.

Absorption of the Ca—HCl complex at different frequencies can be linked with different regions of the potential energy surface and the branching to the different product states is noticeably different. The yield to chemiluminescent products is only important for excitation of certain regions of the potential surface that cross at a reasonable distance from the equilibrium with a potential surface correlating with an excited ion core $Ca^+\,^2D$. Also it can be expected that the decays of the initially excited state in the case of the local excitation of the calcium and in the latter case of the direct excitation of the charge transfer potential have a different appearance.

The latter excitation of the ionic region in the red will result in immediate Cl abstraction to form CaCl while the local A″ excitation in the same spectral region will necessitate a reasonable rearrangement before the excited CaCl* product is formed. Time-resolved experiments have been conducted on the Ca–HBr system within the $Ca(4s4p\,^1P_1)$ region and a 200 fs decay time of the initially excited complex has been observed. This confirms the local nature of the excited state of the calcium. The 200 fs decay might correspond to time necessary to reach the transition state from the Franck–Condon region.

4.3.1.6. *Ground state products from locally excited reactions in alkali metals.* The detection of non-fluorescent ground states within a large population distribution is a difficult problem, as we have just seen for Ca—HCl. A new and general method has been proposed by the group of Polanyi to address this problem in clusters. Here also the reacting system composed of a metal and a molecule or an aggregate of molecules is prepared in a locally excited state of the metal yielding short-lived quasi-bound states whose resonances are analysed to unravel the electron transfer reaction.

The equivalent of an absorption spectrum of the short-lived reaction complex can be measured by depletion spectroscopy. The absorption spectrum of the reacting intermediate is monitored via the decrease of the ground state population of the ground state van der Waals complex of the reagents due to the reaction from the excited state. The major advantage of this method compared with laser-induced fluorescence, used in the preceding section, is being sensitive to electron transfer reactions of non-chemiluminescent or non-luminescent reaction products. This occurs especially in the case of polyatomic molecules such as fluorobenzene or methyl fluoride and hydrogen fluoride with sodium [240–242].

The method yields the detection of the sum of all decay channels of the excited state, reactive or due to electronic energy relaxation of the excited metal. It has, however, the major advantage of yielding directly absolute excitation cross-sections, by measuring the dependence of the ion signal on the intensity of a depletion laser. The absorption cross-section is directly derived from the relative disappearance of the ion signal as

$$\log\left(\frac{N_0}{N}\right) = \sigma_{\text{depletion}}\, F \tag{21}$$

where F is the laser fluence expressed in photons per unit area [243]. This cross-section is directly related to the $\mathrm{I} \rightarrow \mathrm{f}$ absorption and the $\mathrm{f} - \alpha\mathrm{E}$ decay process [244]:

$$\sigma_{\text{dep}} = \frac{4\pi^2\omega}{c} \mid \mu_{\text{if}} \mid^2 \frac{\Gamma_{\text{f}}}{(E - E_{\text{f}})^2 + \Gamma_{\text{f}}^2} \tag{22}$$

Where μ_{if} is the $\mathrm{I} \rightarrow \mathrm{f}$ transition dipole moment and

$$\Gamma_{\text{f}} = \pi \mid \langle \mathrm{f} \mid V \mid \alpha E \rangle \mid^2 \tag{23}$$

represents the linewidth derived from the golden rule expression for the $\mathrm{f} - \alpha E$ decay. This formulation of σ_{dep} is similar to the intensity in the action spectra derived in the case of $Hg–Cl_2$ where it is assumed that all the excited molecules have reacted.

Moreover, using high laser fluences one can saturate the $\mathrm{i} \rightarrow \mathrm{f}$ transition in a manner that depends on the excited state lifetime. Measuring the energy saturation threshold will relate directly to the decay time of this accessed reactive excited state: a long decay will correspond to low saturation threshold and the converse.

Quite a few systems have been investigated this way: $Na_2 \cdots ClCH_3$, $Na_2 \cdots (ClCH_3)_2$, $Na \cdots FPh$ [240, 245], $Na \cdots CH_3X$ [246, 247], $Na \cdots (FCH_3)_n$ $(n = 1 - 4)$ [241], $Li \cdots (FCH_3)$ [248], $Na \cdots HF$ [242*, 249], $Li \cdots HF$ [250]. The photoinduced charge transfer dissociation spectra observed for these systems all reveal the local nature of the excitation. In the case of $Na \cdots (FCH_3)_n (n = 1 - 4)$, for each value of n three broad peaks appear on the red and blue sides of the sodium

D line. As before the interaction of $Na(3p\ ^2P_j)$ with CH_3F results in the formation of the electronic excited states of excited sodium perturbed by CH_3F: $|\Lambda = 1/2, \Omega = 1/2>$, $|\Lambda = 3/2, \Omega = 1/2>$, $|\Lambda = 3/2, \Omega = 3/2>$. Vibrational structure is most prominent for the largest complexes with a spacing of $270\,cm^{-1}$, a value common to strongly bound van der Waals clusters.

A relatively large cross-section ($1.2\,Å^2$) was obtained for the photodepletion excited $Na\cdots(FCH_3)$ complex; this seems indicative of a very favourable geometry for reaction. It compares with a negligible cross-section for reaction in collisions within crossed beams [60]. The reasonably high value of the cross-section, if due to the reaction, implies that the electron transfer can proceed without a barrier. If the electron affinity of the CH_3F molecule were that of the free molecule, there would be a very high barrier at *c.* 6 eV. This suggests that the F—CH_3 bond be substantially released at the transition state to accommodate the electron and to allow a crossing of the ionic potential Na—$(FCH_3)^-$ with the van der Waals one at the distance R_{Na-FCH_3} at *c.* 3 Å, close to the Franck–Condon excitation region accessed from the ground state complex. The increase in the electron affinity in stretching the F—CH_3 bond can be understood; the electron affinity must reach +3.45 eV (atomic fluorine) at infinite distance, starting from −6.2 eV in the molecule. This case is particularly significant in the light of the discussion in section 3.4, where the multidimensional aspect of the harpoon mechanism was introduced. Since it is not absolutely sure that this experiment records purely the reactive channel, it would be very interesting to reproduce the experiment with NaF product detection rather than simply the depletion of the $Na\cdots CH_3F$ complex.

The prototypical $Na\cdots HF$ system has been investigated by the same method. It represents an excellent example, where elaborate and accurate calculations (MRDCI) [251–253] are possible for the ground and excited states of the complex. Also the reaction is best activated by electronic excitation since it is endoergic by *c.* 1.3 eV. The depopulation spectrum represented in figure 12 displays two bands, a small one at 780 nm and a strong one at 650 nm in the immediate red of the sodium D line. In contrast with the preceding case of $Na\cdots FCH_3^*$, there are only two bands in the depopulation spectrum instead of three and the spectrum also extends over a considerable range. There is an extensive vibrational structure within these bands. The calculations reproduce with great accuracy the position of the bands, their shape and the detailed vibrational structure. These bands have in essence the same origin as in the case of $Na\cdots CH_3F$ and result from the interaction of excited $Na(3p\ ^2P)$ with HF, which is very strong in this case and explains the extent of the spectrum over an eV. It is interesting to note the geometries of the three states: the lowest energy state $\tilde{A}(2A')$ of quasi-diatomic symmetry Σ correlates with $Na(3p\ ^1p_2)$ is bound by 0.53 eV and bent at 60°; in contrast, the next two degenerate states, B(3A′,1A″), correlating with $Na(3p\ ^3p_2)$, are linear and bound by 0.34 eV. The geometry changes between the ground state (0.076 eV) and the excited states account for the extensive vibrational structure in both the Na—FH stretch and the bends.

The dynamics of the photoreactive intermediate is quite complex and still need to be elaborated in details. There is a strong avoided crossing, the locus of the electron transfer between the exciplex $\tilde{A}(2A')$ state and the ground X state where the reaction occurs. Dynamical calculations show [254] that the system is trapped in the excited $\tilde{A}(2A')$ exciplex before undergoing a non-adiabatic relaxation to the ground state and that this relaxation is quantal owing to the large energy gap between the two states. The calculations also show the very long lifetime of the excited state (several

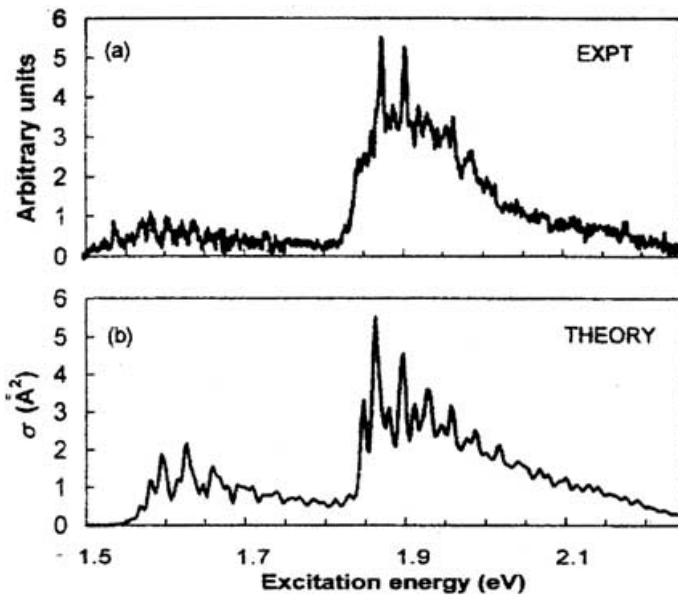

Figure 12. (*a*) Experimental photodepletion spectrum of the Na···FH complex; (*b*) calculated absorption spectrum assuming $T = 250\,\mathrm{K}$. Adapted from [252].

hundred picoseconds), which can be dramatically decreased by the H/D isotope effect and excitation of the HF vibration. A complex process appears where conical intersections come into play to funnel the system from the B to the $\tilde{A}$ state and the avoided crossing further funnels the excited reagents to the ground state. The reactive process can no longer be understood as a classical process leading through a crossing between the electron transfer potential and the initial covalent one to the reaction products; it also involves a non-adiabatic process. Importantly the H—F vibration needs to be activated in the non-adiabatic process to the ground state surface, since the reaction requires some HF stretch as in the preceding case of Na—CH_3F. The question of the access to ground state HF modes and their lifetime has been discussed by Piecuch and co-workers [252, 253].

5. Reaction dynamics at the contact of a reaction medium

A growing literature is concerned with reaction dynamics when the reaction system is embedded in, or located at, the surface of a reaction medium. Most studies concern reaction at the surface of a reaction medium, either the rigid surface of a crystalline or polycrystalline solid [255, 256] or the softer surface of a rare gas cluster [257, 258]. In both cases, the motivation is to identify which forces are at play in heterogeneous chemistry. This issue is very important given that most chemistry occurs in condensed phases.

We mostly focus on surface reactions performed by the cluster isolated chemical reaction (CICR) technique developed in our laboratory [257, 259–262]. The idea is to deposit a controlled number of reactants at the surface of a large van der Waals cluster and to study the dynamics of the reaction that occurs at the surface of the cluster. The results obtained by this technique for metal atom reactions are reviewed

here in the light of related work that does not necessarily involve metal atom reactions. The fact that the reaction proceeds at the surface of a reaction medium rather than in the gas phase under the single-collision regime may change the dynamics in several ways that are discussed now.

5.1. *Changing the approach between reactants*

The surface of the reaction medium reduces the dimensionality of the approach between the reactants, first by switching the approach into two-dimensional instead of three-dimensional space and second and more subtly by forcing the spatial orientation of the reactants.

Polanyi and co-workers first proposed to use this effect to modify access to the TS region of simple $A + BC \rightarrow AB + C$ abstraction reactions, in order to limit the number of impact parameters that are accessible to the system and hence to learn something about the most favourable geometry of the ABC system to access the transition state of the reaction [255, 256, 263]. However, even with a careful choice of both the reaction system (none of the systems studied so far concerns metal atom reactions) and the surface (isolating surfaces were chosen), such experiments can hardly document the reaction as in the absence of a perturbing medium except for the preparation of the collision between reactants. The surface indeed, when interacting strongly enough with the reactant to block reactant geometries, also affects the dynamics of the reaction. Hence, such experiments, rather than documenting the dynamics of the reaction itself, document medium effects on the dynamics of the reaction. This new direction is illustrated by the more recent work from the group of Polanyi that is described below.

5.2. *Changing the access to the TS region*

The previous section has focused the attention on forces that are active before the reaction to block the relative geometry of the reactants. Similarly, the presence of the reaction medium can also change the access to the TS region of the reaction by forcing the spatial orientation of one or several chemical groups forming the reaction system.

This effect is not very likely in the full collision between a reactant pair at the surface of the reaction medium for reasons that will appear below. In contrast, it was observed in TSS studies when the reactant pair is held together and stabilized in a geometry close to that of the TS, before the reaction is turned on by photoexcitation or by photodetachment. For example, when performing a TSS study of the $I + HI$ reaction in a photodetachment experiment where the IHI^- anions are bonded to several argon atoms, the geometry of the IHI^- anion appears perturbed in larger argon clusters and the access to the TS region is changed [258]. Similarly, when turning on the $Ca + HBr \rightarrow CaBr + H$ reaction by photoexcitation of the $Ca \cdots HBr$ complex on $Ar_{\approx 2000}$ clusters, the equilibrium geometry of the complex is slightly bent, whereas it is linear in the gas phase. That causes an easier approach between Ca^* and Br [264].

5.3. *Adding forces in the course of the reaction*

As said above, we do not expect that the presence of the reaction surface changes significantly the access to the TS region of direct reactions that proceed from a full collision at the surface of a rare gas cluster such as those studied in our laboratory [257]. The reason is based on time-scale considerations. The collision

time for direct reactions is of the order of a few picoseconds or smaller. Because of the weakness of the van der Waals modes of the rare gas cluster, the cluster surface has no time to rearrange and the reaction proceeds in a fairly constant force field due to the cluster surface. If the weakness of the forces between reactants and rare gases is considered, this force field is not expected to affect the crossing of the TS region dramatically, and little momentum is exchanged. Of course, this consideration does not apply in the exit valley of the reaction where the cluster has time to rearrange about the products, which can even stay solvated within the cluster.

These expectations are consistent with available observations on the chemiluminescent reaction $Ba + N_2O \rightarrow BaO^* + N_2$ which was studied at the surface of helium droplets [265] and neon [262, 266], argon [266, 267] and N_2 [268] clusters. The product BaO is mostly ejected outside the cluster when the reaction proceeds on helium or neon surfaces. The chemiluminescence spectrum is close to that observed in the gas phase reaction, indicating that the dynamics of the reaction is similar. With argon, a more strongly interacting reaction medium, both free and solvated BaO products are observed, but the chemiluminescence spectrum of the free product is still close to that observed in the gas phase reaction, again indicating similar reaction dynamics. In contrast to the vibrationally and rotationally hot free product, the solvated BaO product is cold because its internal excitation has had time to be quenched by the cluster. Progressive embedding of the BaO product in the interior of the cluster has also been observed [266]. Interestingly, the $Ba + N_2O \rightarrow BaO^* + N_2$ reaction has also been studied in an argon matrix. Of course, only the solvated product was found and it is cold vibrationally [269]. The role of the reaction medium in the ejection of product is considered below.

This question of time-scale in reaction dynamics is quite important and has been studied theoretically in a different context, the dynamics of bimolecular reactions in solution [270]. Direct atom exchange reactions that proceed across an activation barrier were considered and the solvent was a rare gas fluid. Its role is important at the foothill of the potential barrier, prior to reaction, where the solvent has time to 'prepare' the impulse given to the reactants to surmount the reaction barrier. Conversely, the solvent is not active in the TS region of the reaction, except at high solvent pressure or with more strongly interacting solvents than rare gas fluids [270, 271]. We are thus very far from the simple picture of a reaction medium applying a constant friction along the reaction path.

In the case where the reaction system carries significant multipolar moments in the TS region that do not exist in the reactant or product side, then the reaction medium could act as a solvating medium along the reaction coordinate, by lowering the transition state energy as does a catalyst in heterogeneous chemistry. This could be especially important when the reaction medium consists of polar molecules. In that case the force field exerted by the reaction medium along the reaction coordinate can change significantly in the TS region, with consequences for the reaction dynamics. To our knowledge, such situations have not been investigated yet, although they could represent interesting microscopic models of catalysts. In this perspective, the question of time-scale could be crucial for excited state metal atom reactions where reactions must proceed on the excited surface, before the energy is lost in other channels. If the reaction is made easier by surrounding solvent molecules which lower the barrier to reaction, then electronic relaxation can be overrun and the reaction proceed more easily.

5.4. *Acting as a heat bath*

Owing to its very large number of degrees of freedom, the reaction medium can be considered as a heat bath that is more or less well coupled to the reacting system on its way to products. However, since reaction dynamics considers phenomena at the microscopic level, heat bath effects should be reduced to collision effects between the reacting system and atom or molecules constituting the reaction medium. These collisions result in additional forces, unknown in the gas phase, that affect the dynamics of the reaction. For this reason the present section is simply a continuation of the preceding one.

As formerly mentioned, collisions with the substrate occur mostly in the exit channel from the product recoil and can result in the stabilization of the reacting system in secondary wells of the potential energy surface as was observed for the Ba–Cl_2 system where the $BaCl_2$ intermediate was observed [272]. In the exit channel of the reaction, collisions with the substrate can either result in solvation of the reaction product (discussed in the previous section) or simply affect the angular and energy distribution of the product that is ejected in the gas phase. This effect has not been studied in metal atom reactions but was documented extensively for the photodissociation of molecules (mostly hydrogen halides) dissociating either from argon clusters [273–275] or from the surface of macroscopic crystals. Several ejection pathways were identified for the photofragments, the importance of which depends on the surface coverage. The ejection is termed 'direct' when the photoproduct escapes the surface without collisions. In that case the product has a similar energy distribution to that in gas phase photodissociation. The ejection is 'inelastic' when the photoproduct experiences one or several collisions before escaping. At significant surface coverage, the ejection can be 'indirect' and involves an exchange reaction between the primary photoproduct which not observed and a molecule of the absorbed layer [276–280].

The possibility of using the interaction with the cluster surface to stabilize the reactive system in a secondary well was brought up by the unexpected observation that a small energy barrier prevents the electron transfer in the harpooning reactions $Ba + CO_2 \rightarrow BaO + CO$ and $Ba + SF_6 \rightarrow BaF + SF_5$. A single barium atom has been deposited with either a single CO_2 or a single SF_6 molecule at the surface of an argon cluster of average size 6000 [259, 281]. No reaction was observed at the cluster temperatures, although exothermic reaction channels are accessible and have been observed in crossed-beam experiments (for instance that of Herm *et al.* for the $Ba + SF_6$ reaction [282]). This was interpreted as due to a small barrier in the entrance channel of the reaction which precludes electron transfer at the cluster temperature (32 K [283]) but which can be overcome at collision energies of 0.1 eV as in crossed-beam collisions. Presumably the barrier is due to a short-distance electron transfer. In contrast, small barium clusters react with these molecules, i.e. two or more Ba molecules with CO_2 and three or more Ba molecules with SF_6, suggesting that the entrance barrier drops below an energy that is accessible at the cluster temperature. This can be rationalized qualitatively with the help of the harpoon model by considering that small barium clusters have a smaller ionization energy than the barium atom [284] and therefore moves the electron jump to larger distances.

5.5. *The $Ca\cdots HBr(Ar)_n$ reaction*

The TSS of the reaction

$$\underbrace{Ca\cdots HBr}_{\substack{\text{ground state}\\ \text{van der Waals}\\ \text{complex}}} \quad \underbrace{h\nu}_{\substack{\text{photoinduction}\\ \text{of the reaction}}} \quad \underbrace{[Ca^{*}\cdots HBr \rightsquigarrow Ca^{+}(HBr)^{-}]}_{\text{TS region}} \longrightarrow \underbrace{CaBr^{*} + H}_{\substack{\text{chemiluminescent}\\ \text{products}}} \tag{24}$$

has been performed with the $Ca\cdots HBr$ complex (called the 'surface complex' hereafter) deposited on the surface of Ar_{2000} clusters according to the CICR technique [264, 285]. This reaction has been studied before when the $Ca\cdots HBr$ complex (called the 'free complex' hereafter) is free in the gas phase [231]. The comparison between both experiments serves now to illustrate several aspects discussed above concerning the effect of the cluster environment on reaction dynamics.

According to the CICR technique and considering that the cluster temperature (32 K [283]) is small compared with the binding energy of the $Ca\cdots HBr$ complex, the single Ca atom and the single HBr molecule that are deposited on the same Ar_{2000} cluster are free to migrate, to collide with each other and to form the complex, the excess energy being evacuated in the numerous degrees of freedom of the argon cluster. The experiment consists in turning on the reaction by excitation of calcium near the resonance line and observing the reaction by recording the chemiluminescence of the product CaBr. The main experimental observation is an action spectrum where the chemiluminescence signal is monitored while scanning the laser that turns on the reaction. It is complemented by the analysis of the chemiluminescence spectrum.

The action spectrum recorded in the cluster experiment is shown in the top panel of figure 13. The experimental data are represented by points and error bars. The full curve smooths the experimental points in order to show the structure of the spectrum.

On the basis of the considerations of the previous sections, the interpretation of these data assumes that the accessibility to the TS region is not totally transformed by the argon cluster. Hence a reminiscence of the 'free complex' action spectrum must be found in the spectrum of the 'surface complex'. The structured part of the 'surface complex' spectrum might be the expected reminiscence as suggested by the bottom panel of the figure where the dotted curve labelled 'simulated' has been obtained as follows: the gas phase action spectrum has been blue shifted by 90 cm^{-1} and has been added to a broad unsymmetrical component peaking in the blue, which is shown as a broken curve in the bottom panel of figure 13.

The resemblance between the simulated curve and the experimental one for the 'surface complex' is striking, although differences exist. Of course the effect of the cluster environment on the dynamics of the reaction is contained in these differences, in the shift of the 'free complex' spectrum and in the presence of the broad component. Two different classes of effects have been distinguished in [285] depending on whether the entrance or the exit channels of the reaction are considered.

In the entrance channel of the reaction, the cluster can act geometrically by changing the shape of the complex (taking the linear shape of the gas phase complex as a reference) or dynamically by inducing forces in the reacting system. The former

effect does not seem to be very important. This is revealed by the need for the 'free complex' spectrum to be blue shifted to match the simulated curve with the experimental 'surface complex' curve in the bottom panel of figure 13. The second effect shows up in changing the shape of the action spectrum. In particular, the presence of the cluster seems to add a component to the action spectrum, absent when the reaction is photoinduced in a free Ca···HBr complex. It may correspond to the excited 4p orbital of calcium pointing towards the cluster surface and forcing a movement perpendicular to the cluster surface, i.e. perpendicular to the HBr

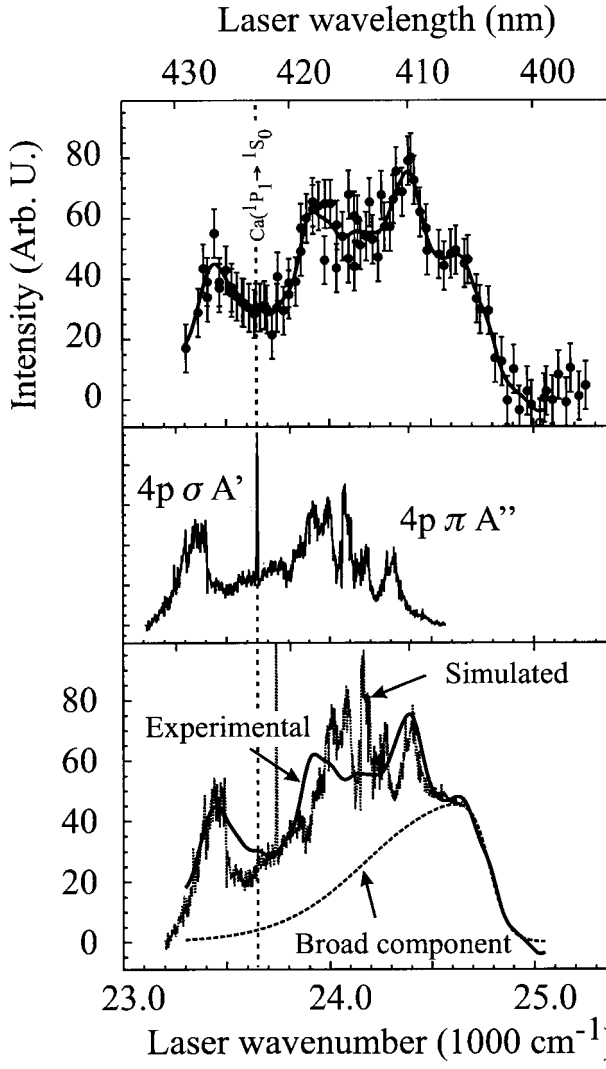

Figure 13. Action spectrum of the Ca + HBr reaction in the 'surface complex' experiment (top panel). The full curve smooths the experimental points. The action spectrum taken in the 'free complex' experiment is shown in the middle panel and is adapted from [239]. The bottom panel compares the 'surface complex' experiment (shown as the full curve smoothing the experimental data of the top panel) with a simulation where the 'free complex' action spectrum of the middle panel is blue shifted by 90 cm^{-1} and added to the broad component shown as a broken curve in the figure.

molecule which is mostly parallel to the cluster surface, which cannot be achieved when the Ca···HBr complex is not supported at the cluster surface. This effect is instantaneous on excitation of the 4p orbital of calcium and does not need rearrangement of the cluster surface to operate.

In the exit channel of the reaction, the cluster acts by quenching the electronic, vibrational and rotational energy of the product CaBr. Nevertheless, the quenching is partial. Some of the CaBr product remains electronically excited with a vibrational temperature much larger than the cluster temperature (1000–1700 K versus 32 K), hence suggesting that the ejection of the product CaBr in the gas phase is far from a thermal evaporation outside the cluster surface.

6. Real-time movements about the TS region

Exploring the surface in time during the course of the reaction has been made possible by the advent of femtochemistry [10, 286, 287]. Essentially a pump laser prepares the reactants in a selected region of the potential energy surface and a well-chosen probe monitors the advance of the reaction at certain crucial steps: the reaction complex, the transition region and the final products. The typical example in bimolecular reactions is the attack of CO_2 by atomic hydrogen where an intermediate HOCO had been characterized by Wittig and co-workers [213]. Indeed the excitation of the $IH \cdots CO_2$ complex reveals this transient [288]. In excited metal reactions, time domain experiments should be of the highest importance in order to characterize several aspects of the evolution:

- Is it possible to bring into evidence the moment at which the charge transfer region is traversed?
- What is the electronic and vibrational configuration of the parents?
- What is the branching ratio to electronically excited states in the products and how is energy redistributed over possible electronic states?

There have been few experiments on bimolecular complexes and even fewer on metal–molecule excited complexes, essentially by the groups of Radloff and Gonzáles Urena [289–292] on the $Ba \cdots FCH_3$ van der Waals complex. The depletion spectrum of this binary complex reflects the absorption spectrum and exhibits resonances [293]. One of the most prominent ones at 618 nm is diffuse and should correspond to the origin of an electronic transition $\tilde{A}$ correlating with $Ba(^1P_1) + CH_3F$. It has been ascribed a lifetime of *c.* 250 fs from linewidth measurements. The direct excitation with a femtosecond laser of this resonance yields an equivalent 270 fs decay time for the excited complex as measured by a depletion technique. This surprisingly 'long' evolution time has been further investigated by photoelectron–photoion coincidence detection. The photoelectron spectrum coincident with the product BaF formation detected with a 400 nm probe laser has revealed a double peak with a 0.35 eV separation. The higher energy peak is assigned to the ionization of $Ba \cdots FCH_3$ followed by reaction within the corresponding ion. The low energy component thus corresponds to the ionization of the neutral BaF product. The authors have concluded that there is an indirect reaction path with an induction step of the reaction via internal conversion from the optically accessed state of the complex $\tilde{A}$ correlating with $Ba(^1P_1) + CH_3F$ to a lower state $\tilde{A}'$ correlating with $Ba(^1D_2)$. This step also yields in parallel the unreacted excited

$Ba(^1D_2)$. From the analysis of the results a typical reaction time of 50 ($\pm$30) fs has been found yielding electronically excited BaF, probably in the B state.

Thus the reaction time is short, *c.* 50 fs, which agrees with a rapid downhill descent to the products. However, the indirect mechanism of electronic relaxation prior to reaction is a surprise since the reaction should also be direct in the $\tilde{A}$ state. In addition, the reaction in the $\tilde{A}'$ state is very rapid in order to compete with the direct dissociation channel into $Ba(^1D_2) + CH_3F$. The latter channel can be directly excited by a laser at 795 nm [292]. This reactivity following non-adiabatic energy flow in the excited complex has also been characterized in time-independent studies by Polanyi for the Na $\cdots$ HF complex where only the lowest electronically excited state $2\,^2A'$ is observed to lead to the ground state product NaF. Saturation measurements performed by this group on selected lines of this complex have revealed a rather long lifetime which in turn points to a reaction on the ground state surface controlled in time by non-adiabatic crossing to the $1\,^2A'$ surface.

7. Epilogue

Through this review we have progressed from the early one-dimensional harpoon model of Polanyi [1, 2], which accounts for alkali–halogen reactions, to a multi-dimensional view of the transition state, necessary for describing the reactions of alkaline earth metals with oxidants, for example. This arises from the fact that the electron jump cannot occur instantly owing to a low electron affinity of the oxidant and this requires the stretch of a bond connecting to a halogen or an oxygen atom to increase its affinity. This has been known for a long time but becomes more or less unavoidable when more complex reactions of metals with oxidants are explored and should now be amenable to direct observation. The idea of a simple electron jump is really too coarse for metals beyond sodium, because the electron jump of one electron when it occurs drives the reaction but the properties of the transition state and the energy distribution of the products (electronic, vibrational) rely on the non-transferred electron. Indeed the chemistry is that of the non-harpoon electron; see for example all the reactions of excited metal atoms. We have also reviewed the methods to characterize the TS: crossed-beam scattering, TSS and now the upcoming femto-TSS. All methods have their advantages: the first is a general-purpose tool, while TSS spectroscopy gives high precision information on a zone determined by Franck–Condon factors and allows initiation of the reaction from selected regions therefrom. Now femto-TSS has the additional advantage of initiating the reaction from a region from where the reaction can be followed up to the final products, signalling the presence of one or several transition states, in principle.

This prospect relies on the development of efficient techniques to monitor sudden changes in the electronic nature of potential surfaces, by electron ion coincidences between selected products and the relevant time-resolved photoelectron spectra [294–297]. This should help in describing the surfaces that are traversed on the way to the products but should also allow the direct characterization of the previously mentioned stretching of the electron acceptor coordinate and to which position the electron hops. Femtochemistry focuses on the observation of the movements with a pump–probe scheme with the shortest possible pulse duration. The reacting system is set free to evolve after the preparation pulse. On the contrary, optimal control seeks to amplify movements of the reacting system to force its way to

products. One is, in principle, able to retrieve the information on the relevant modes to describe the PES of the reaction around the transition state. The idea of using teaching procedures to shape the intensity, the wavelength and the phase of laser pulses optimally to control chemical reactions was proposed theoretically 10 years ago by Judson and Rabitz [298]. This technique was applied first to the multiphoton ionization of the $Fe(CO)_5$ and $CpFe(CO)_2Cl$ molecules [299]. In particular, it was demonstrated that an evolutionary algorithm could be used to optimize the laser pulse in order to maximize the $CpFe(CO)Cl^+ : FeCl^+$ branching ratio without any *a priori* knowledge of the system and of its potential surfaces. This technique has been used successfully to control the branching of various photofragmentation processes to several channels [300–303]. Of course, optimum control can be considered as a way of maximizing the yield of particularly interesting reactions, but the reverse prospect is also interesting. Indeed, if the optimized laser pulse is able to improve substantially the yield of a reaction, then its intensity, wavelength and phase profiles contain information about the dynamics of the reaction that is optimized. This leads to the problem of inversion, i.e. the question of obtaining information on reaction dynamics from pulse shape analysis, a field that is only at its beginning [301, 303–305]. Impressively, it has been shown in a photoionization study of Na_nK_p clusters that optimized pulses for NaK^+ consist in a train of peaks that relate to wavepacket propagation, the spacing between peaks corresponding to integer or half-integer numbers of the vibrational period of NaK [301]. This way of getting insight into wavepacket motions in the TS region of a reaction is still in its infancy, and to our knowledge has not been applied yet to bimolecular reactions. However, is it quite conceivable to step in this direction and to use this technique for optimizing reactions such as $Ca^* + HCl \rightarrow CaCl^* + H$ using the $Ca \cdots HCl$ van der Waals complex to put the reactants close to the TS region of the reaction. Dynamical stereochemistry, which suffered from interactions in the entrance valley of a reaction scrambling alignment, could find here its realm with the activation of special internal coordinates or intermolecular coordinates by forced oscillations with the laser.

Finally, the observation of transition states in the presence of a medium is an essential direction in the future since one endeavours here to influence the course of the reaction of a metal by passive methods. Here again the femto-TSS approach should be essential.

References

[1] Eyring, H., and Polanyi, M., 1931, *Z. phys. Chem.* B, **12**, 279.
[2] Polanyi, M., 1932, *Atomic Reactions* (London: Williams and Northgate).
[3] Eller, K., and Schwarz, H., 1991, *Chem. Rev.*, **91**, 1121.
[4] Weisshaar, J. C., 1993, *Acc. chem. Res.*, **26**, 213.
[5] Capron, L., Mestdagh, H., and Rolando, C., 1998, *Coord. Chem. Rev.*, **180**, 269.
[6] Rodgers, M. T., and Armentrout, P. B., 2000, *Mass Spectrum. Rev.*, **19**, 215.
[7] Lindinger, W., Hansel, A., and Herman, Z., 2000, *Adv. at. mol., opt. Phys.*, **43**, 243.
[8] Eyring, H., 1935, *J. chem. Phys.*, **3**, 107.
[9] Laidler, K. J., and King, M. C., 1983, *J. phys. Chem.*, **87**, 2657.
[10] Polanyi, J. C., and Zewail, A. H., 1995, *Acc. chem. Res.*, **28**, 119.
[11] Truhlar, D. G., Garrett, B. C., and Klippenstein, S. J., 1996, *J. phys. Chem.*, **100**, 12771.
[12] Wigner, E., 1938, *Trans. Faraday Soc.*, **34**, 29.
[13] Petersson, G. A., 2000, *Theor. Chem. Acc.*, **103**, 190.

[14] Garrett, B. C., 2000, *Theor. Chem. Acc.*, **103**, 200.
[15] Bohr, N., and Wheeler, J. A., 1939, *Phys. Rev.*, **86**, 426.
[16] Baer, T., and Hase, W. L., 1996, *Unimolecular Reaction Dynamics: Theory and Experiments* (New York: Oxford University Press).
[17] Polanyi, J. C., and Wong, W. H., 1969, *J. chem. Phys.*, **51**, 1439.
[18] Mok, M. H., and Polanyi, J. C., 1969, *J. chem. Phys.*, **51**, 1451.
[19] Polanyi, J. C., 1972, *Acc. chem. Res.*, **5**, 161.
[20] Polanyi, J. C., 1987, *Chem. Scr.*, **27**, 229.
[21] Bonnet, L., and Rayez, J. C., 1997, *J. phys. Chem.* A, **101**, 9318.
[22] Bonnet, L., and Rayez, J. C., 1998, *Eur. Phys. J.* D, **4**, 169.
[23] Bonnet, L., and Rayez, J. C., 1999, *Phys. Chem. chem. Phys.*, **1**, 2383.
[24] Bonnet, L., and Rayez, J. C.., 1999, *J. chem. Phys.*, **110**, 4772.
[25] Polanyi, J. C., and Schreiber, J. L., 1974, in *Physical Chemistry, An Advanced Treatise,* Vol. 6-A, edited by W. Jost (New York: Academic), pp. 383–487.
[26] Herschbach, D. R., 1976, *Pure appl. Chem.*, **47**, 61.
[27] Herm, R. R., 1979, in *Alkali Halide Vapors, Structure, Spectra and Reaction Dynamics* edited by P. Davidovits and D. McFadden (New York: Academic), Chap. 7, pp. 189–253.
[28] Levy, M. R., 1979, *Prog. React. Kinet.*, **10**, 1.
[29] Zare, R. N., and Bernstein, R. B., 1980, *Phys. Today*, **33**, 43.
[30] Bersohn, R., 1986, *NATO ASI Ser.* C, **184**, 21.
[31] Herschbach, D. R., 1987, *Chem. Scr.*, **27**, 327.
[32] Lee, Y. T., 1987, *Science*, **236**, 793.
[33] Lee, Y. T., 1987, *Chem. Scr.*, **27**, 215.
[34] González Ureña, A., and Vetter, R., 1995, *J. Chem. Soc. Faraday Trans.*, **91,** 389.
[35] González Ureña, A., and Vetter, R., 1996, *Int. Rev. phys. Chem.*, **15**, 375.
[36] Casavecchia, P., Balucani, N., and Volpi, G. G., 1999, *Annu. Rev. phys. Chem.*, **50**, 347.
[37] Magee, J. L., 1940, *J. chem. Phys.*, **8**, 687.
[38] Gislason, E. A., 1979, in *Alkali Halide Vapors, Structure, Spectra and Reaction Dynamics*, edited by P. Davidovits and D. McFadden (New York: Academic), Chap. 13, p. 415.
[39] Truhlar, D. G., and Dixon, D. A., 1979, in *Atom–Molecule Collision Theory: a Guide for the Experimentalist*, edited by R. B. Bernstein (NewYork: Plenum), Chap. 18, 595–646.
[40] Herm, R. R., and Herschbach, D. R., 1970, *J. chem. Phys.*, **52**, 5783.
[41] Grice, R., 1995, *Int. Rev. phys. Chem.*, **14**, 315.
[42] Herschbach, D. R., 1966, in *Advances in Chemical Physics*, Vol. X, edited by I. Prigogine (New York: Wiley), pp. 319–393.
[43] Bernstein, R. B., Herschbach, D. R., and Levine, R. D., 1987, *J. phys. Chem.*, **91**, 5365.
[44] Song, J.-B., Gislason, E. A., and Sizun, M., 1995, *J. chem. Phys.*, **103**, 4885.
[45] Kuntz, P. J., Nemetz, E., and Polanyi, J. C., 1969, *J. chem. Phys.*, **50**, 4607.
[46] Kuntz, P. J., Mok, E. H., and Polany, J. C., 1969, *J. chem. Phys.*, **50**, 4623.
[47] Kuntz, P. J., 1969, *Trans. Faraday Soc.*, **66**, 2980.
[48] Kuntz, P. J., 1972, *Mol. Phys.*, **23**, 1035.
[49] Wiskerke, A. E., Stolte, S., Loesch, H. J., and Levine, R. D., 1999, *Phys. Chem. chem. Phys.*, **2**, 757.
[50] Herschbach, D. R., 1973, *Faraday Discuss. Chem. Soc.*, **55**, 233.
[51] Prisant, M. G., Rettner, C. T., and Zare, R. N., 1984, *J. chem. Phys.*, **81**, 2699.
[52] Loesch, H. J., and Moeller, J., 1997, *J. phys. Chem.* A, **101**, 7534.
[53] Loesch, H. J., 1995, *Annu. Rev. phys. Chem.*, **46**, 555.
[54] Loesch, H. J., and Stienkemeier, F., 1993, *J. chem. Phys.*, **98**, 9570.
[55] Banares, L., and González Ureña, A., 1990, *J. chem. Phys.*, **93**, 6473.
[56] Ding, G., Yang, W., Sun, W., Xu, D., He, G., and Lou, N., 1994, *Chem. Phys. Lett.*, **220**, 1.
[57] Hennessy, R. J., Ono, Y., and Simons, J. P., 1981, *Mol. Phys.*, **43**, 181.
[58] Siska, P. E., and Herschbach, D. R., 1994, *Can. J. Chem.*, **72**, 762.

[59] Choi, S. E., and Bernstein, R. B., 1985, *J. chem. Phys.*, **83**, 4463.
[60] Weiss, P. S., Schmidt, H., Covinsky, M. H., Lee, Y. T., and Mestdagh, J. M., 1991, *J. phys. Chem.*, **95**, 3005.
[61] Hertel, I. V., 1982, *Adv. chem. Phys.*, **50**, 475.
[62] Mestdagh, J.-M., Balko, B. A., Covinsky, M. H., Weiss, P. S., Vernon, M. F., Schmidt, H., and Lee, Y. T., 1987, *Faraday Discuss*, **84**, 145.
[63] Vernon, M. F., Schmidt, P., Weiss, H., Covinsky, M. H., and Lee, Y. T., 1986, *J. chem. Phys.*, **84**, 5580.
[64] Weiss, P. S., Mestdagh, J.-M., Covinsky, M. H., Balko, B. A., and Lee, Y. T., 1988, *Chem. Phys.*, **126**, 93.
[65] Case, D. A., and Herschbach, D. R., 1975, *Mol. Phys.*, **30**, 1537.
[66] Case, D. A., and Herschbach, D. R., 1976, *J. chem. Phys.*, **64**, 4212.
[67] Case, D. A., and Herschbach, D. R., 1978, *J. chem. Phys.*, **69**, 150.
[68] McClelland, G. M., and Herschbach, D. R., 1979, *J. phys. Chem.*, **83**, 1445.
[69] Lindsay, D. M., Symons, M. C. R., Herschbach, D. R., and Kwiram, A. L., 1982, *J. chem. Phys. Chem.*, **86**, 3789.
[70] Brooks, P. R., 1995, *Int. Rev. Chem.*, **14**, 327.
[71] Harris, S. A., Wiediger, S. D., and Brooks, P. R., 1999, *J. phys. Chem.* A, **103**, 10035.
[72] Harris, S. A., Harland, P. W., and Brooks, P. R., 2000, *Phys. Chem. chem. Phys.*, **2**, 787.
[73] Brooks, P. R., 1969, *J. chem. Phys.*, **50**, 5031.
[74] Marcelin, G., and Brooks, P. R., 1975, *J. Am. Chem. Soc.*, **97**, 1710.
[75] Brooks, P. R., 1976, *Science*, **193**, 11.
[76] Brooks, P. R., McKillop, J. S., and Pippin, H. G., 1979, *Chem. Phys. Lett.*, **66**, 144.
[77] Beuhler, R., Jr., and Bernstein, R. B., 1969, *J. chem. Phys.*, **51**, 5305.
[78] Parker, D. H., Chakravorty, K. K., and Bernstein, R. B., 1981, *J. phys. Chem.*, **85**, 466.
[79] Parker, D. H., Chakravorty, K. K., and Bernstein, R. B., 1982, *Chem. Phys. Lett.*, **86**, 289.
[80] Bernstein, R. B., 1985, *J. chem. Phys.*, **82**, 3656.
[81] Parker, D. H., and Bernstein, R. B., 1989, *Annu. Rev. phys. Chem.*, **40**, 561.
[82] Gandhi, S. R., and Bernstein, R. B., 1990, *J. chem. Phys.*, **93**, 4024.
[83] Jalink, H., Harren, F., Van den Ende, D., and Stolte, S., 1986, *Chem. Phys.*, **108**, 391.
[84] Stolte, S., 1982, *Ber. Bunsenges. phys. Chem.*, **86**, 413.
[85] Jalink, H., Parker, D. H., Meiwes-Broer, K. H., and Stolte, S., 1986, *J. phys. Chem.*, **90**, 552.
[86] Stolte, S., 1988, in *Atomic and Molecular Beam Methods*, edited by G. Scoles (Oxford: Oxford University Press), Volume 1, Chapter 25, pp. 631–652.
[87] Jalink, H., Janssen, M. H. M., Geijsberts, M., and Stolte, S., 1988, *NATO ASI Ser.* C, **245**, 195.
[88] Jalink, H., Nicolasen, G., Stolte, S., and Parker, D. H., 1989, *J. Chem. Soc. Faraday Trans. 2*, **85**, 1115.
[89] Janssen, M. H. M., Parker, D. H., and Stolte, S., 1997, *J. phys. Chem.*, **95**, 8142.
[90] Bulthuis, J., and Stolte, S., 1997, *J. phys. Chem.*, **95**, 8180.
[91] Bulthuis, J., Milan, J. B., Janssen, M. H. M., and Stolte, S., 1991, *J. chem. Phys.*, **94**, 7181.
[92] Vrakking, M. J. J., and Stolte, S., 1997, *Chem. Phys. Lett.*, **271**, 209.
[93] Loesch, H. J., and Remscheid, A., 1991, *J. phys. Chem.*, **95**, 8194.
[94] Loesch, H. J., and Moeller, J. J., 1992, *Chem. Phys.*, **97**, 9016.
[95] Loesch, H., and Moller, J., 1999, *Faraday Discuss.*, **113**, 241.
[96] Alonso, J., Banares, L., Menendez, M., and González Ureña, A., 1988, *Can. J. Chem.*, **66**, 1410.
[97] Levine, R. D., 1990, *Chem. Phys. Lett.*, **175**, 331.
[98] Levine, R. D., 1990, *J. Phys. Chem.*, **94**, 8872.
[99] Weiss, P. S., Covinsky, M. H., Schmidt, H., Balko, B. A., Lee, Y. T., and Mestdagh, J.-M., 1988, *Z. Phys.* D, **10**, 227.

[100] Düren, R., Lackschewitz, U., and Milosevic, S., 1990, *Rev. sci. Instrum.*, **61**, 1064.
[101] Düren, R., Lackschewitz, U., Milosevic, S., and Waldapfel, H. J., 1990, *Chem. Phys.*, **140**, 199.
[102] Rettner, C. T., and Zare, R. N., 1981, *J. chem. Phys.*, **75**, 3636.
[103] Rettner, C. T., and Zare, R. N., 1982, *J. chem. Phys.*, **77**, 2416.
[104] Suits, A. G., Hou, H., and Lee, Y. T., 1990, *J. phys. Chem.*, **94**, 5672.
[105] Suits, A. G., Hou, H., Davis, H. F., and Lee, Y. T., 1992, *J. chem. Phys.*, **96**, 2777.
[106] Ding, G., Sun, W., Yang, W., Xu, D., He, G., and Lou, N., 1999, *Mol. Phys.*, **96**, 1349.
[107] Hertel, I. V., Schmidt, H., Baehring, A., and Meyer, E., 1985, *Rep. Prog. Phys.*, **48**, 375.
[108] Ben-Nun, M., Martinez, T. J., and Levine, R. D., 1997, *J. phys. Chem.* A, **101**, 7522.
[109] Orr-Ewing, A. J., and Zare, R. N., 1995, in *The Chemical Dynamics and Kinetics of Small Radicals*, edited by L. K. Wagner and A. Wagner (Singapore: World Scientific), Volume 2, Chapter 20, pp. 936–1063.
[110] Zhan, J. P., Yang, H. P., Deng, W. Q., and Lou, N. Q., 1997, *J. phys. Chem.* A, **101**, 7486.
[111] Garay, M., Menendez, M., Verdasco, E., Castano, J., and González Ureña, A., 1993, *J. phys. Chem.*, **97**, 5836.
[112] Garay, M., Esteban, E., Verdasco, M., and González Ureña, A. 1995, *Chem. Phys.*, **195**, 235.
[113] Orea, J. M., Laplaza, A., Rinaldi, C. A., Tardajos, G., and González Ureña, A., 1997, *Chem. Phys.*, **220**, 337.
[114] Weast, R. C., Astle, M. J., and Beyer, W. H., 1984, *Handbook of Chemistry and Physics*, 65th Edn (Boca Raton, FL: CRC Press).
[115] Davis, H. F., Suits, A. G., and Lee, Y. T., 1992, in *Gas-Phase Metal Reaction*, edited by A. Fontijn (Amsterdam: North-Holland), pp. 319–347.
[116] Menzinger, M., 1985, in *Gas-Phase Chemiluminescence and Chemi-Ionization*, edited by A. Fontijn (Amsterdam: Elsevier), pp. 25–66.
[117] Menzinger, M., 1988, *Acta Phys. Pol.* A, **73**, 85.
[118] Whitehead, J. C. in *Comprehensive Chemical Kinetics*, Vol. 24, *Modern Methods in Kinetics* (Amsterdam: Elsevier), Chap. 5, pp. 357–506.
[119] Jonah, C. D., and Zare, R. N., 1971, *Chem. Phys. Lett.*, **9**, 65.
[120] Lin, S. M., Mims, C. A., and Herm, R. R., 1973, *J. chem. Phys.*, **58**, 327.
[121] Dagdigian, P. J., 1985, in *Gas-Phase Chemiluminescence and Chemi-Ionization*, edited by A. Fontijn (Amsterdam: Elsevier), pp. 203–219.
[122] Davis, H. F., Suits, A. G., Hou, H., and Lee, Y. T., 1990, *Ber. Bunsenges. phys. Chem.*, **94**, 1193.
[123] Suits, A. G., Hou, H., Davis, H. F., and Lee, Y. T., 1991, *J. phys. Chem.*, **95**, 8207.
[124] Suits, A. G., Hou, H., Floyd David, H., Lee, Y. T., and Mestdagh, J. M., 1991, *J. chem. Phys.*, **95**, 8178.
[125] Banares, L., and González Ureña, A., 1992, *THEOCHEM*, **90**, 271.
[126] Kierzkowski, P., and Kowalski, A., 2000, *Eur. Phys. J.* D, **12**, 487.
[127] Rice, S. F., Martin, H., and Field, R. W., 1985, *J. chem. Phys.*, **82**, 5023.
[128] De Castro, M., Candori, R., Pirani, F., Aquilanti, V., Garay, M., and González Ureña, A., 1998, *J. phys. Chem.* A, **102**, 9537.
[129] De Castro, M., Candori, R., Pirani, F., Aquilanti, V., Garay, M., and González Ureña, A., 2000, *J. chem. Phys.*, **112**, 770.
[130] De Castro Vitores, M., Candori, R., Pirani, F., Aquilanti, V., Ménendez, M., Garay, M., and González Ureña, A., 1996, *J. phys. Chem.*, **100**, 7997.
[131] Garay Salazar, M., Orea Rocha, J. M., González Ureña, A., and Roberts, G., 1999, *Mol. Phys.*, **97**, 967.
[132] Los, J., and Kleyn, A. W., 1979, in *Alkali Halide Vapors, Structure, Spectra and Reaction Dynamics*, edited by P. Davidovits and D. McFadden (New York: Academic), Chap. 8, pp. 275–330.
[133] Kleyn, A. W., Khromov, V. N., and Los, J., 1980, *J. chem. Phys.*, **72**, 5282.
[134] Kleyn, A. W., Khromov, V. N., and Los, J., 1980, *Chem. Phys.*, **52**, 65.

[135] KLEYN, A. W., GISLASON, E. A., and LOS, J., 1980, *Chem. Phys.*, **52**, 81.
[136] ONEIL, S. V., ROSMUS, P., and NORCROSS, D. W., 1986, *J. chem. Phys.*, **85**, 7232.
[137] ČÍŽEK, M., HORÁČEK, J., and DOMCKE, W., 1999, *Phys. Rev.* A, **60**, 2873.
[138] ČÍŽEK, M., HORÁČEK, J., SERGENTON, A. C., POPOVÍC, D. B., ALLAN, M., DOMCKE, W., LEININGER, T., and GADEA, F. X., 2001, *Phys. Rev.* A, **63**, 062710-1--14.
[139] HUBER, K. P., and HERZBERG, G., 1979, *Molecular Spectra and Molecular Structure. IV. Constants of Diatomic Molecules* (New York: van Nostrand).
[140] GAUYACQ, J. P., 1986, *Europhys. Lett.*, **1**, 287.
[141] DAVIS, H. F., SUITS, A. G., and LEE, Y. T., 1992, *J. chem. Phys.*, **96**, 6710.
[142] CHEONG, B. S., and PARSON, J. M., 1994, *J. chem. Phys.*, **100**, 2637.
[143] FLOYD DAVIS, H., SUITS, A., LEE, Y. T., ALCARAZ, C., and MESTDAGH, J. M., 1993, *J. chem. Phys.*, **98**, 959.
[144] OBERLANDER, M. D., KAMPF, R. P., and PARSON, J. M., 1997, *Chem. Phys. Lett.*, **176**, 385.
[145] PARSON, J. M., and FANG, C. C., 1990, *J. chem. Phys.*, **92**, 4823.
[146] FANG, C. C., and PARSON, J. M., 1991, *J. chem. Phys.*, **95**, 6413.
[147] BALTAYAN, P., HARTMANN, F., HIKMET, I., PEBAY-PEYROULA, J. C., and SADEGHI, N., 1989, *Chem. Phys. Lett.*, **160**, 549.
[148] BALTAYAN, P., HARTMANN, F., HIKMET, I., and SADEGHI, N., 1992, *J. chem. Phys.*, **97**, 5417.
[149] HIKMET, I., KOWALCZYK, P., and SADEGHI, N., 1992, *Chem. Phys. Lett.*, **188**, 287.
[150] KOWALCZYK, P., HIKMET, I., and SADEGHI, N., 1992, *Chem. Phys.*, **160**, 73.
[151] SADEGHI, N., HIKMET, I., COLOMB, I., and SETSER, D. W., 1992, in *Gas-Phase Metal Reaction*, edited by A. Fontijn (Amsterdam: North-Holland), pp. 363–392.
[152] LEVY, M. R., 1991, *J. phys. Chem.*, **95**, 8500.
[153] LEVY, M. R., 1991, *J. phys. Chem.*, **95**, 8491.
[154] HERBERTSON, D. L., NEWNHAM, D. A., and LEVY, M. R., 1994, *Can. J. Chem.*, **72**, 850.
[155] NEWNHAM, D. A., and LEVY, M. R., 1996, *J. phys. Chem.*, **100**, 2799.
[156] HERBERTSON, D. L., and LEVY, M. R., 1996, *J. phys. Chem.*, **100**, 2809.
[157] HERBERTSON, D. L., and LEVY, M. R., 1996, *J. phys. Chem.*, **100**, 14584.
[158] SPENCE, M. A., and LEVY, M. R., 1997, *J. phys. Chem.*, A, **101**, 7490.
[159] HUGHES, T. J., and LEVY, M. R., 2000, *Phys. Chem. chem. Phys.*, **2**, 651.
[160] SPENCE, M. A., TOMLINSON, W. R., and LEVY, M. R., 2001, *Phys. Chem. chem. Phys.*, **3**, 3610.
[161] SPENCE, M. A., TOMLINSON, W. R., and LEVY, M. R., 2001, *Phys. Chem. chem. Phys.*, **3**, 3622.
[162] LEVY, M. R., 1993, *Res. chem. Kinet.*, **1**, 163.
[163] SALEM, L., 1982, *Electrons in Chemical Reactions: First Principles* (New York: Wiley).
[164] JEAN, Y., VOLATRON, F., and BURDETT, J., 1993, *An Introduction to Molecular Orbitals* (New York: Oxford University Press).
[165] LABINGER, J. A., and BERCAW, J. E., 2002, *Nature*, **417**, 507.
[166] GREEN, K. M., KAMPF, R. P., and PARSON, J. M., 2000, *J. chem. Phys.*, **112**, 1721.
[167] VETTER, R., NAULIN, C., and COSTES, M., 2000, *Phys. Chem. chem. Phys.*, **2**, 643.
[168] LUC, P., and VETTER, R., 2001, *J. chem. Phys.*, **115**, 11106.
[169] JEUNG, G. H., LUC, P., VETTER, R., KIM, K. H., and LEE, Y. S., 2002, *Phys. Chem. chem. Phys.*, **4**, 596.
[170] RITTER, D., CARROLL, J. J., and WEISSHAAR, J. C., 1992, *J. phys. Chem.*, **96**, 10636.
[171] CARROLL, J. J., WEISSHAAR, J. C., SIEGBAHN, P. E. M., WITTBORN, C. A. M., and BLOMBERG, M. R. A., 1995, *J. phys. Chem.*, **99**, 14388.
[172] CARROLL, J. J., HAUG, K. L., WEISSHAAR, J. C., BLOMBERG, M. R. A., SIEGBAHN, P. E. M., and SVENSSON, M., 1995, *J. phys. Chem.*, **99**, 13955.
[173] CARROLL, J. J., and WEISSHAAR, J. C., 1996, *J. phys. Chem.*, **100**, 12355.
[174] WEN, Y., POREMBSKI, M., FERRETT, T. A., and WEISSHAAR, J. C., 1998, *J. phys. Chem.*, A, **102**, 8362.
[175] POREMBSKI, M., and WEISSHAAR, J. C., 2000, *J. phys. Chem.* A, **104**, 1524.
[176] POREMBSKI, M., and WEISSHAAR, J. C., 2001, *J. phys. Chem.* A, **105**, 4851.

[177] Willis, P. A., Stauffer, H. U., Hinrichs, R. Z., and Davis, H. F., 1998, *J. chem. Phys.*, **108**, 2665.
[178] Willis, P. A., Stauffer, H. U., Hinrichs, R. Z., and Davis, H. F., 1998, *SPIE*, **3271**, 72.
[179] Willis, P. A., Stauffer, H. U., Hinrichs, R. Z., and Davis, H. F., 1999, *J. phys. Chem.* A, **103**, 3706.
[180] Stauffer, H. U., Hinrichs, R. Z., Schroden, J. J., and Davis, H. F., 1999, *J. chem. Phys.*, **111**, 10758.
[181] Stauffer, H. U., Hinrichs, R. Z., Willis, P. A., and Davis, H. F., 1999, *J. chem. Phys.*, **111**, 4101.
[182] Willis, P. A., Stauffer, H. U., Hinrichs, R. Z., and Davis, H. F., 1999, *Rev. sci. Instrum.*, **70**, 2606.
[183] Hinrichs, R. Z., Willis, P. A., Stauffer, H. U., Schroden, J. J., and Davis, H. F., 2000, *J. chem. Phys.*, **112**, 4634.
[184] Stauffer, H. U., Hinrichs, R. Z., Schroden, J. J., and Davis, H. F., 2000, *J. phys. Chem.* A, **104**, 1107.
[185] Blomberg, M. R. A., Siegbahn, P. E. M., and Svensson, M., 1992, *J. phys. Chem.*, **96**, 9794.
[186] Wittborn, A. M. C., Costas, M., Blomberg, M. R. A., and Siegbahn, P. E. M., 1997, *J. chem. Phys.*, **107**, 4318.
[187] Dewar, M., 1951, *Bull. Soc. Chim.*, **18**, C71.
[188] Atkins, P. W., 1995, *Physical Chemistry*, 5th Edn (Oxford: Oxford University Press).
[189] Porembski, M., and Weisshaar, J. C., 2001, *J. phys. Chem.* A, **105**, 6655.
[190] Arrowsmith, P., Bartoszek, F. E., Bly, S. H. P., Carrington, J., Charters, T. P. E., and Polanyi, J. C., 1980, *J. chem. Phys.*, **73**, 5859.
[191] Polanyi, J. C., and Wolf, R. J., 1981, *J. chem. Phys.*, **75**, 5951.
[192] Foth, H. J., Polanyi, J. C., and Telle, H. H., 1982, *J. phys. Chem.*, **86**, 5027.
[193] Gallagher, A., 1982, in *Spectral Line Shapes*, Vol. 2, edited by K. Burnett (Berlin: De Gruyter), p. 755.
[194] Hering, P., Brooks, P. R., Curl, Jr, R. F., Judson, R. S., and Lowe, R. S., 1980, *Phys. Rev. Lett.*, **44**, 687.
[195] Maguire, T. C., Brooks, P. R., and Curl, R. F., 1983, *Phys. Rev. Lett.*, **50**, 1918.
[196] Maguire, T. C., Brooks, P. R., Curl, R. F., Spence, J. H., and Ulvick, S. J., 1986, *J. chem. Phys.*, **85**, 844.
[197] Kaesdorf, S., Brooks, P. R., Curl, R. F., Spence, J. H., and Ulvick, S. J., 1986, *Phys. Rev.* A, **34**, 4418.
[198] Brooks, P., 1998, *Chem. Rev.*, **88**, 407.
[199] Barnes, M. D., Brookes, P. R., Curl, R. F. Jr, and Harland, P. W., 1991, *J. chem. Phys.*, **94**, 5245.
[200] Barnes, M. D., Brooks, P. R., Curl, R. F., Harland, P. W., and Johnson, B. R., 1992, *J. chem. Phys.*, **96**, 3559.
[201] Kleiber, P. D., Lyyra, A. M., Sando, K. M., Heneghan, S. P., and Stwalley, W. C., 1985, *Phys. Rev. Lett.*, **54**, 2003.
[202] Kleiber, P. D., Lyyra, A. M., Sando, K. M., Zafiropoulos, V., and Stwalley, W. C., 1986, *J. chem. Phys.*, **85**, 5493.
[203] Bililign, S., and Kleiber, P. D., 1990, *Phys. Rev.* A, **42**, 6838.
[204] Bililign, S., and Kleiber, P. D., 1992, *J. chem. Phys.*, **96**, 213.
[205] Bililign, S., Kleiber, P. D., Kearney, W. R., and Sando, K. M., 1992, *J. chem. Phys.*, **96**, 218.
[206] Wong, T. H., and Kleiber, P. D., 1995, *J. chem. Phys.*, **102**, 6476.
[207] Wong, T. H., Freel, C., Kleiber, P. D., and Sando, K. M., 1998, *J. chem. Phys.*, **108**, 5723.
[208] Wong, T. H., Kleiber, P. D., and Yang, K. H., 1999, *J. chem. Phys.*, **110**, 6743.
[209] Rossi, F., and Pascale, J., 1985, *Phys. Rev.* A, **32**, 2657.
[210] Jouvet, C., and Soep, B., 1983, *Chem. Phys. Lett.*, **96**, 426.
[211] Jouvet, C., and Soep, B., 1985, *J. Physique* C1, **46**, 313.
[212] Reisler, H., and Wittig, C., 1986, *Annu. Rev. phys. Chem.*, **37**, 307.

[213] Shin, S. K., Chen, Y., Nickolaisen, S., Sharpe, S. W., Beaudet, R. A., and Wittig, C., 1991, *Adv. Photochem.*, **16**, 249.
[214] Neumark, D. M., 1992, *Annu. Rev. phys. Chem.*, **43**, 153.
[215] Weaver, A., Metz, R. B., Bradforth, S. E., and Neumark, D. M., 1988, *J. phys. Chem.*, **92**, 5558.
[216] Metz, R. B., Bradforth, S. E., and Neumark, D. M., 1992, in *Advances in Chemical Physics*, Vol. 81, edited by I. Prigogine and S. A. Rice (New York: Wiley), pp. 1–61.
[217] Neumark, D. M., 1996, *Science*, **272**, 1446.
[218] Bradforth, S. E., Weaver, A., Arnold, D. W., Metz, R. B., and Neumark, D. M., 1990, *J. chem. Phys.*, **92**, 7205.
[219] Strobel, A., Fischer, I., Lochschmidt, A., Müller-Dethlefs, K., and Bondybey, V. E., 1994, *J. phys. Chem.*, **98**, 2024.
[220] Breckenridge, W. H., Jouvet, C., and Soep, B., 1986, *J. chem. Phys.*, **84**, 1443.
[221] Jouvet, C., Boivineau, M., Duval, M. C., and Soep, B., 1987, *J. phys. Chem.*, **91**, 5416.
[222] Shin, S. K., Chen, Y., Nickolaisen, S., Sharpe, S. W., Beaudet, R. A., and Wittig, C., 1991, in *Advances in Photochemistry*, Vol. 16, edited by D. Volman, G. Hammond and D. Neckers (New York: Wiley), pp. 249–363.
[223] Qin, J., and Setser, D. W., 1991, *Chem. Phys. Lett.*, **184**, 121.
[224] Qin, J., Nelson, T. O., and Setser, D. W., 1991, *J. phys. Chem.*, **95**, 5374.
[225] Huang, F., Setser, D. W., and Cheong, B. S., 1994, *Isr. J. Chem.*, **34**, 127.
[226] Backhaus, P., Schmidt, B., and Dantus, M., 1999, *Chem. Phys. Lett.*, **306**, 18.
[227] Olson, R. E., Smith, E. T., and Bauer, E., 1971, *Appl. Opt.*, **10**, 1848.
[228] Bernstein, R. B., Herschbach, D. R., and Levine, R. D., 1987, *J. phys. Chem.*, **91**, 5365.
[229] Keller, A., Lawruszczuk, R., Soep, B., and Visticot, J., 1996, *J. chem. Phys.*, **105**, 4556.
[230] Keller, A., Visticot, J. P., Tsuchiya, S., Zwier, T. S., Duval, M. C., Jouvet, C., Soep, B., and Whitham, C., 1990, in *Dynamics of Polyatomic van der Waals Complexes*, Vol. 227, *NATO ASI Series*, edited by N. Halberstadt and K. C. Janda (New York: Plenum), pp. 103–121.
[231] Soep, B., Abbès, S., Keller, A., and Visticot, J. P., 1992, *J. chem. Phys.*, **96**, 440.
[232] Lawruszczuk, R., Elhanine, M., and Soep, B., 1998, *J. chem. Phys.*, **108**, 8374.
[233] Menendez, M., Garay, M., Verdasco, E., and González Ureña, A., 1993, *J. Chem. Soc. Faraday Trans.*, **89**, 1493.
[234] Dubernet, M. L., and Hutson, J. M., 1994, *J. chem. Phys.*, **101,** 1939.
[235] Soep, B., Whitham, C., Keller, A., and Visticot, J. P., 1991, *Faraday Discuss. Chem. Soc.*, **91**, 191.
[236] De-Castro-Vittores, M., Candori, M. R., Pirani, F., Aquilanti, V., Menendez, M., Garay, M., and González Ureña, A., 1996, *J. phys. Chem.*, **100**, 7997.
[237] De-Castro-Vittores, M., Candori, M. R., Pirani, F., Aquilanti, V., Garray, M., and González Ureña, A., 1998, *J. phys. Chem.*, **10**, 9537.
[238] De-Castro-Vittores, M., Candori, M. R., Pirani, F., Aquilanti, V., Garay, M., and González Ureña, A., 2000, *J. chem. Phys.*, **112**, 770.
[239] De-Castro-Vittores, M., Candori, M. R., Pirani, F., Aquilanti, V., Garay, M., and González Ureña, A., 1996, *Chem. Phys. Lett.*, **263**, 456.
[240] Liu, K., Polanyi, J., and Yang, S. H., 1993, *J. chem. Phys.*, **98**, 5431.
[241] Polanyi, J., and Wang, J.-X., 1995, *J. phys. Chem.*, **99**, 13691.
[242] Topaler, M. S., Truhlar, D. G., Chang, X. Y., Piecuch, P., and Polanyi, J. C., 1998, *J. chem. Phys.*, **108**, 5349.
[243] Buck, U., 1990, *Dynamics of Polyatomic van der Waals Complexes, Nato ASI Series*, Vol. B227, edited by N. Halberstadt and K. C. Janda (New York: Plenum).
[244] Beswick, J. A., 1987, *NATO ASI Ser.*, **212**, 563.
[245] Liu, K., Polanyi, J. C., and Yang, S., 1992, *J. chem. Phys.*, **96**, 8628.
[246] Polanyi, J., Wang, J. X., and Yang, S. H., 1994, *Isr. J. Chem.*, **34**, 55.
[247] Chang, X. Y., Ehlich, R., Hudson, A. J., Polanyi, J., and Wang, J. X., 1997, *J. chem. Phys.*, **106**, 3988.

[248] Hudson, A. J., Naumkin, F. Y., Oh, H. B., Polanyi, J. C., and Raspopov, S. A., 2001, *Faraday Discuss.*, **118**, 191.
[249] Chang, X. Y., Ehlich, R., Hudson, A. J., Piecuch, P., and Polanyi, J., 1997, *Faraday Discuss.*, **108**, 411.
[250] Hudson, A. J., Oh, H. B., Polanyi, J. C., and Piecuch, P., 2000, *J. chem. Phys.*, **113**, 9897.
[251] Topaler, M. S., Truhlar, D. G., Chang, X. Y., Piecuch, P., and Polanyi, J. C., 1998, *J. chem. Phys.*, **108**, 5378.
[252] Spirko, V., Piecuch, P., and Bludsky, O., 2000, *J. chem. Phys.*, **112**, 189.
[253] Mrugala, F., Piecuch, P., Spirko, V., and Bludsky, O., 2000, *J. mol. Struct.*, **555**, 43.
[254] Zeiri, Y., Katz, G., Kosloff, R., Topaler, M., Truhlar, D., and Polanyi, J., 1999, *Chem. Phys. Lett.*, **300**, 523.
[255] Barnes, J. A., Polanyi, J. C., Reiland, W., and Thomas, D. F., 1984, *J. chem. Phys.*, **82**, 3824.
[256] Polanyi, J. C., and Williams, R. J., 1988, *J. chem. Phys.*, **88**, 3363.
[257] Mestdagh, J. M., Gaveau, M. A., Gée, C., Sublemontier, O., and Visticot, J. P., 1997, *Int. Rev. phys. Chem.*, **16**, 215.
[258] Liu, Z., Gómez, H., and Neumark, D. M., 2001, *Faraday Discuss.*, **118**, 221.
[259] Gée, C., Gaveau, M. A., Sublemontier, O., Mestdagh, J. M., and Visticot, J. P., 1997, *J. chem. Phys.*, **107**, 4194.
[260] Gaveau, M. A., Briant, M., Fournier, P. R., Mestdagh, J. M., and Visticot, J. P., 2000, *Phys. Chem. chem. Phys.*, **2**, 831.
[261] Briant, M., Gaveau, M. A., Mestdagh, J. M., and Visticot, J. P., 2000, *J. chem. Phys.*, **112**, 1744.
[262] Gaveau, M.-A., Briant, M., Vallet, V., Mestdagh, J.-M., and Visticot, J.-P., 2001, in *Atomic and Molecular Beams, The State of the Art*, edited by R. Campargue (Berlin: Springer).
[263] Cho, C. C., Polanyi, J. C., and Stanners, C. D., 1989, *J. chem. Phys.*, **90**, 598.
[264] Briant, M., Gaveau, M. A., Fournier, P. R., Mestadagh, J. M., Visticot, J. P., and Soep, B., 2001, *Faraday Discuss.*, **118**, 209.
[265] Lugovoj, E., Toennies, J. P., and Vilesov, A., 2000, *J. chem. Phys.*, **112**, 8217.
[266] Gaveau, M., Briant, M., Fournier, P., Mestdagh, J., and Visticot, J., 2000, *Phys. Chem. chem. Phys.*, **2**, 831.
[267] Lallement, A., Mestdagh, J. M., Meynadier, P., de Pugo, P., Sublemontier, O., Visticot, J. P., Berlande, J., Biquard, X., Cuvellier, J., and Hickman, C. G., 1993, *J. chem. Phys.*, **99**, 8705.
[268] Gée, C., Gaveau, M., Mestdagh, J., Osborne, M., Sublemontier, O., and Visticot, J., 1996, *J. phys. Chem.*, **100**, 13421.
[269] Long, S. R, Lee, Y. P., Krogh, O. D., and Pimentel, G. C., 1982, *J. chem. Phys.*, **77**, 226.
[270] Ben-Nun, M., and Levine, R. D., 1992, *J. chem. Phys.*, **97**, 8341.
[271] Charutz, D. M., and Levine, R. D., 1993, *J. chem. Phys.*, **98**, 1979.
[272] Biquard, X., Sublemontier, O., Berlande, J., Gaveau, M. A., Mestdagh, J. M., Schilling, B., and Visticot, J. P., 1995, *J. Chimie phys.*, **92**, 264.
[273] Slavicek, P., Zdanska, P., Jungwirth, P., Baumfalk, R., and Buck, U., 2000, *J. phys. Chem.* A, **104**, 7793.
[274] Baumfalk, R., Nahler, N. H., Buck, U., Niv, M. Y., and Gerber, R. B., 2000, *J. chem. Phys.*, **113**, 329.
[275] Baumfalk, R., Nahler, N. H., and Buck, U., 2001, *Faraday Discuss.*, **118**, 247.
[276] Polanyi, J. C., and Zeiri, Y., 1995, in *Laser Spectroscopy and Photochemistry on Metal Surfaces*, edited by H. L. Dai and W. Ho. (Singapore: World Scientific), p. 1241.
[277] Giorgi, J. B., Kühnemuth, R., and Polanyi, J., 1999, *J. chem. Phys.*, **110**, 598.
[278] Lee, T. G., Liu, W., and Polanyi, J. C., 1999, *Surf. Sci.*, **426**, 173.
[279] Giorgi, J. B., Naumkin, F. Y., Polanyi, J. C., Raspopov, S. A., and Sze, N. K., 2000, *J. chem. Phys.*, **112**, 9569.
[280] Giorgi, J. B., Kuhnemuth, R., and Polanyi, J. C., 2000, *J. chem. Phys.*, **113**, 807.

[281] Visticot, J., Gaveau, M., Eulry, P., Lengaigne, M., Mestdagh, J., and Gée, C., 1997, *Faraday Discuss.*, **108**, 401.
[282] Herm, R. R., Lin, S. M., and Mims, C. A., 1973, *J. phys. Chem.*, **77**, 2931.
[283] Farges, J., de Feraudy, M. F., Raoult, B., and Torchet, G., 1986, *J. chem. Phys.*, **84**, 3491.
[284] Boutou, V., Allouche, A. R., Spiegelmann, F., Chevaleyre, J., and Aubert Frécon, M., 1998, *Eur. Phys. J.* D, **2**, 63.
[285] Briant, M., Fournier, P. R., Gaveau, M. A., Mestdagh, J. M., Soep, B., and Visticot, J. P., 2002, *J. chem. Phys.*, **117**, 5036.
[286] Dantus, M., Rosker, M. J., and Zewail, A. H., 1987, *J. chem. Phys.*, **87**, 2395.
[287] Zewail, A. H., 1995, in *Femtosecond Chemistry*, edited by J. Manz and L. Wöste (Weinheim: VCH), pp. 15–128.
[288] Scherer, N. F., Sipes, C., Bernstein, R. B., and Zewail, A. H., 1990, *J. chem. Phys.*, **92**, 5239.
[289] Farmanara, P., Stert, V., Radloff, W., Skowronek, S., and González Ureña, A., 1999, *Chem. Phys. Lett.*, **304**, 127.
[290] Stert, V., Farmanara, P., Radloff, W., Noack, F., Skowronek, S., and González Ureña, A., 1999, *Phys. Rev.* A, **59**, R1727.
[291] Stert, V., Farmanara, P., Ritze, H.-H., Radloff, W., and González Ureña, A., 2001, *Chem. Phys. Lett.*, **337**, 299.
[292] Stert, V., Ritze, H. H., Farmanara, P., and Radloff, W., 2001, *Phys. Chem. chem. Phys.*, **3**, 3939.
[293] Skowronek, S., Jiménez, J. B., and González Ureña, A., 1999, *J. chem. Phys.*, **111**, 460.
[294] Davies, J. A., Leclaire, J. E., Continetti, R. E., and Hayden, C. C., 1999, *J. chem. Phys.*, **111**, 1.
[295] Davies, J. A., Continetti, R. E., Chandler, D. W., and Hayden, C. C., 2000, *Phys. Rev. Lett.*, **84**, 5983.
[296] Blanchet, V., Zgierski, M. Z., Seideman, T., and Stolow, A., 1999, *Nature*, **401**, 52.
[297] Lehr, L., Zanni, M. T., Frischkorn, C., Weinkauf, R., and Neumark, D. M., 1999, *Science*, **284**, 635.
[298] Judson, R. S., and Rabitz, H., 1992, *Phys. Rev. Lett.*, **68**, 1500.
[299] Assion, A., Baumert, T., Bergt, M., Brixner, T., Kiefer, B., Seyfried, V., Stehle, M., and Gerber, G., 1998, *Science*, **282**, 919.
[300] Feurer, T., Glass, A., Rozgonyi, T., Sauerbrey, R., and Szabo, G., 2001, *Chem. Phys.*, **267**, 223.
[301] Bartelt, A., Minemoto, S., Lupulescu, C., Vajda, V., and Wöste, L., 2001, *Eur. Phys. J.* D, **16**, 127.
[302] Daniel, C., Full, J., González, L., Kaposta, C., Krenz, M., Lupulescu, C., Manz, J., Minemoto, S., Oppel, M., Rosendo-Francisco, P., Vadja, V., and Wöste, L., 2001, *Chem. Phys.*, **267**, 247.
[303] Levis, R. J., and Rabitz, H. A., 2002, *J. phys. Chem.* A, **106**, 6427.
[304] Rabitz, H., and Zhu, W. S., 2000, *Acc. chem. Res.*, **33**, 572.
[305] Brixner, T., Kiefer, B., and Gerber, G., 2001, *Chem. Phys.*, **267**, 241.